Spatiotemporal responses in crop water footprint and benchmark under different irrigation techniques to climate change scenarios in China

Zhiwei Yue[1, 3,*], Xiangxiang Ji[1, 3,*], La Zhuo[2, 3, 4, 5], Wei Wang[4,5], Zhibin Li[4,5], Pute Wu[2, 3, 4, 5]

[1]College of Water Resources and Architectural Engineering, Northwest A&F University, Yangling 712100, China
[2]Institute of Soil and Water Conservation, Northwest A&F University, Yangling 712100, China
[3]Institute of Water-saving Agriculture in Arid Regions of China, Northwest A&F University, Yangling 712100, China
[4]Institute of Soil and Water Conservation, Chinese Academy of Sciences and Ministry of Water Resources, Yangling 712100, China
[5] University of Chinese Academy of Sciences, Beijing 100049, China.

*The authors contribute equally.
Correspondence to: La Zhuo (zhuola@nwafu.edu.cn; lzhuo@ms.iswc.ac.cn) and Pute Wu (gjzwpt@hotmail.com)

Abstract. Adaptation to future climate change with limited water resources is a major global challenge to sustainable and sufficient crop production. However, the large-scale responses of crop water footprint and its associated benchmarks under various irrigation techniques to future climate change scenarios remain unclear. The present study quantified the responses of maize and wheat water footprint per unit yield (WF, $m^3 t^{-1}$) and corresponding WF benchmarks under two representative concentration pathways (RCPs) in the 2030s, 2050s, and 2080s at a 5-arc minute grid level in China. The AquaCrop model with the outputs of six global climate models in Coupled Model Intercomparison Project Phase 5 (CMIP5) as its input data was used to simulate the WF of maize and wheat. The differences among rain-fed and furrow-, micro-, and sprinkler-irrigated wheat and maize were identified. Compared with the baseline year (2013), maize WF will increase under both RCP2.6 and RCP8.5, by 17 % and 13 %, respectively, until the 2080s. Wheat WF will increase under RCP2.6 (by 12 % until the 2080s) and decrease by 12 % under RCP8.5 until the 2080s, with a higher increase in wheat yield and decrease in wheat WF due to the higher CO_2 concentration in 2080s under RCP8.5. WF will increase the most for rain-fed crops. Relative to rain-fed crops, micro irrigation and sprinkler irrigation result in the smallest increases in WF for maize and wheat, respectively. These water-saving managements will mitigate the negative impact of climate change more effectively. The WF benchmarks of maize and wheat in the humid zone (~overall average at 680 $m^3 t^{-1}$ for maize and 873 $m^3 t^{-1}$ for wheat at 20th percentile) are 13–32 % higher than those in the arid zone (~ overall average at 601 $m^3 t^{-1}$ for maize and 753 $m^3 t^{-1}$ for wheat). The differences in WF benchmarks among various irrigation techniques are more significant in the arid zone, which can be as high as 57%, for 20th percentile WF benchmarks of 1020 $m^3 t^{-1}$ for sprinkler-irrigated wheat and 648 $m^3 t^{-1}$ for micro-irrigated wheat. Nevertheless, WF benchmarks will not respond to climate changes as dramatically as the WF in the same area, especially in the area with limited agricultural development. The present study demonstrated that the visible different responses to climate change in terms of crop water consumption, water use efficiency, and WF benchmarks under different irrigation techniques cannot be

35 ignored. It also lays the foundation for future investigations into the influences of irrigation methods, RCPs, and crop types on

36 WF and its benchmarks in response to climate change in all agricultural regions worldwide.

37 **1 Introduction**

38   The progressive decline in water resource availability is a major impediment to global food production security (Pastor

39 et al., 2019; Trnka et al., 2019; Konapala et al., 2020). Food crops are the main source of human nutrition (Myers et al., 2017;

40 Lobell and Gourdji, 2012). Humans depend on food crops for ~47 % of their daily protein intake (FAO, 2021). However, as a

41 result of human activity, the climate system is changing and global warming is a significant characteristic of this process (IPCC,

42 2021). Since the 1980s, each successive decade has been warmer than any preceding one after 1850 (Kappelle, 2020). Climate

43 change affects water consumption and crop yield by altering precipitation, temperature, carbon dioxide (CO_2) concentration,

44 and other factors during crop growth (Hatfield and Dold, 2019). Crop adaptation to future climate change with limited water

45 resources has become a major challenge in sustainable crop production and supply worldwide.

46   The water footprint per unit crop (WF, m^3 t^{-1}) (Hoekstra, 2003) is the amount of water consumed by the crop per unit

47 yield during crop growth within a certain region. It includes blue WF (surface and groundwater), green WF (precipitation that

48 will not become runoff), and grey WF (freshwater that assimilates pollutants from human activities) (Hoekstra et al., 2011).

49 Blue and green WF are collectively known as consumptive WF, and grey WF is also called degradative WF (Hoekstra, 2013).

50 Unlike traditional crop water productivity and other agricultural water metrics, WF covers water consumption, sources, and

51 spatiotemporal dimensions during the crop growth period. Therefore, water consumption intensity and efficiency for irrigated

52 and rain-fed growing modes may be compared. WF is an effective indicator of the sustainability of regional water use and

53 optimal water resource allocation (Xu et al., 2019; Mali et al., 2021). The present study focuses exclusively on consumptive

54 WF, which depends on crop yield and the intensity of water consumption per unit planted area.

55   Several studies have been conducted on the responses of WF to future climate change. Nevertheless, no consensus has

56 been reached. Certain scholars believe that future climate change will weaken food crop production security. Ahmadi et al.

57 (2021) reported that maize WF in the Qazvin Plain of India will increase by 42 % and 147 % under representative concentration

58 pathways (RCP) 4.5 and RCP8.5, respectively, by 2061–2080. Zheng et al. (2020) found that rice yield in Henan and Jiangsu

59 Provinces (China) will decrease, while WF will increase under four RCPs at various stages of the 21st century. Other scholars

60 believe that crop yield may actually benefit from future increases in precipitation and atmospheric CO_2 concentration. Jans et

61 al. (2021) considered the combined effects of changes in climatic factors, such as temperature, precipitation, and rising

62 atmospheric CO_2 concentration, and predicted that between 2011 and 2099, global cotton yield will increase by > 50 % and

63 WF will decrease by 30 % under RCP8.5. Arunrat et al. (2020) found that in the present century, the yield of individual and

64 large-scale rice farms in Thailand will increase by 1–30 % and 2–31 %, respectively, while WF will decrease by 10–43 % and

65 1–67 %, respectively, under RCP4.5. Significant spatiotemporal differences in WF under various irrigation techniques have

66 been confirmed at the site (Chukalla et al., 2015) and regional (Wang et al., 2019) scales. However, current large-scale studies

on the responses of WF to environmental change are usually based on simulations assuming adequate furrow irrigation. These studies exclude comparisons between various irrigation techniques and the differences in their influences on crop WFs. Although Dai et al. (2020) optimised maize and wheat cropping patterns under RCP4.5 and RCP8.5 with consideration of various irrigation modes in the Huaihe River Basin in China by 2050, they only considered blue water.

Magnitudes and constitution of crop WF vary widely among regions and areas (Mekonnen and Hoekstra, 2011). To encourage water users to reduce WF to a reasonable level, Hoekstra (2013, 2014) recommended establishing WF benchmarks for different products as they facilitate prudent water allocation and fair water resource sharing among sectors and users (Hoekstra, 2013). On the large-scale, specific WF benchmarks can be set for crops grown on different farms within the same region (Mekonnen and Hoekstra, 2014). A previous study demonstrated the sensitivity of WF benchmarks to climate zones (Zhuo et al., 2016a). WF benchmarks significantly differ among irrigation techniques, especially in arid zones (Wang et al., 2019). However, little is known about the responses of WF benchmarks under different irrigation techniques to future climate change.

To investigate the influence of future climate change on large-scale WF and benchmarks under diverse irrigation techniques, maize and wheat grown in mainland China were the subjects of this study. We used the outputs of six global climate models (GCMs) (Table 1), including three models each for relatively wet and dry climate outputs, in Coupled Model Intercomparison Project Phase 5 (CMIP5). We then used the AquaCrop model to simulate the spatiotemporal responses of blue and green WF and corresponding WF benchmarks for wheat and maize in the 2030s (2020–2049), 2050s (2040–2069), and 2080s (2070–2099) under RCP2.6 and RCP8.5 at a 5-arc minute grid resolution. We distinguished between rain-fed and irrigated growing modes and among furrow, micro, and sprinkler irrigation.

As of 2019, China was the world's second largest maize and largest wheat producer, accounting for 23 % and 17 % of total global production, respectively (FAO, 2021). China's cereal production has helped stabilise global food production and supply. In 2019, the planted areas of maize and wheat in China were 41 million ha and 24 million ha, respectively, and accounted for 25 % and 14 % of the national total croplands, respectively (NBSC, 2021). Cereal production consumes substantial volumes of water in China, and these quantities change over time. Zhuo et al. (2019) reported that maize water consumption increased by 49 % between 2000 and 2013 as planted areas and feed demand increased. Conversely, Wang et al. (2019) reported that wheat planted and irrigated areas decreased and water consumption slightly declined (4.4 %) from 2000 to 2014. Other studies reported that maize and wheat consume relatively more water in the North than the South of China (Tian et al., 2019; Wang et al., 2019). Developing water-saving irrigation has become an important way to alleviate the prominent contradiction between water resources utilization and grain production in China. According to NBSC (2021), the area of water-saving irrigation projects in China in 2019 was 37 million ha, including 7 million ha for micro irrigation. Therefore, micro irrigation does apply to food crops in China despite the limited irrigated area. For instance, in Xinjiang province, the area of micro irrigated maize and wheat was 0.033 million ha in 2009 (CIDDC, 2022), of which the wheat area dominated at up to 0.031 million ha (Wang et al., 2011). Meanwhile, some scholars are conducting research on micro irrigated maize (Bai and Gao, 2021; Guo et al., 2021) and wheat (Li et al., 2021; Zain et al., 2021) in China, especially in the North. Therefore, the

water consumption rates of these staple crops under future climate change scenarios with different irrigation techniques should be closely monitored to ensure water supply and food crop production security in China and worldwide. Compared to existing literatures on evaluation of WFs of crop production under climate change scenarios (e.g., Karandish et al., 2022), the innovations of the current research are embodied in two points. The present study clarifies large-scale spatiotemporal responses of WF to future climate change scenarios under different irrigation techniques for the first time. This analysis is also the first to explore the large-scale future changes in WF benchmarks under different irrigation techniques.

Table 1. Inventory of global climate models (GCMs) used in the current study.

GCM	Institute	Reference	Type
CCCMA-CanESM2	Canadian Centre for Climate Modelling and Analysis	Arora et al. (2011); von Salzen et al. (2013)	Wet
CESM1-CAM5	National Science Foundation, Department of Energy, National Center for Atmospheric Research	Hurrell et al. (2013)	
GFDL-CM3	NOAA Geophysical Fluid Dynamics Laboratory	Delworth et al. (2006); Donner et al. (2011)	
FIO-ESM	The First Institute of Oceanography, State Oceanic Administration, China	Qiao et al. (2013)	Dry
GISS-E2R	NASA Goddard Institute for Space Studies USA	Schmidt et al. (2006); Schmidt et al. (2014)	
IPSL-CM5A-MR	Institute Pierre Simon Laplace	Dufresne et al. (2013)	

2 Method and data

2.1 Research set-up

We studied the spatiotemporal responses of blue and green WF and corresponding WF benchmarks for two crops (maize and wheat) to future climate change under two climate change scenarios (RCP2.6 and RCP8.5) using four different growing modes (rain-fed and furrow-, micro-, and sprinkler-irrigated). First, we determined the baseline year. Second, we considered different growing modes to quantify WF and corresponding WF benchmarks of two crops in the baseline year and future year levels under two climate change scenarios. Finally, the spatiotemporal responses of crop WF and corresponding WF benchmarks to future climate change were analysed (Fig. 1).

120
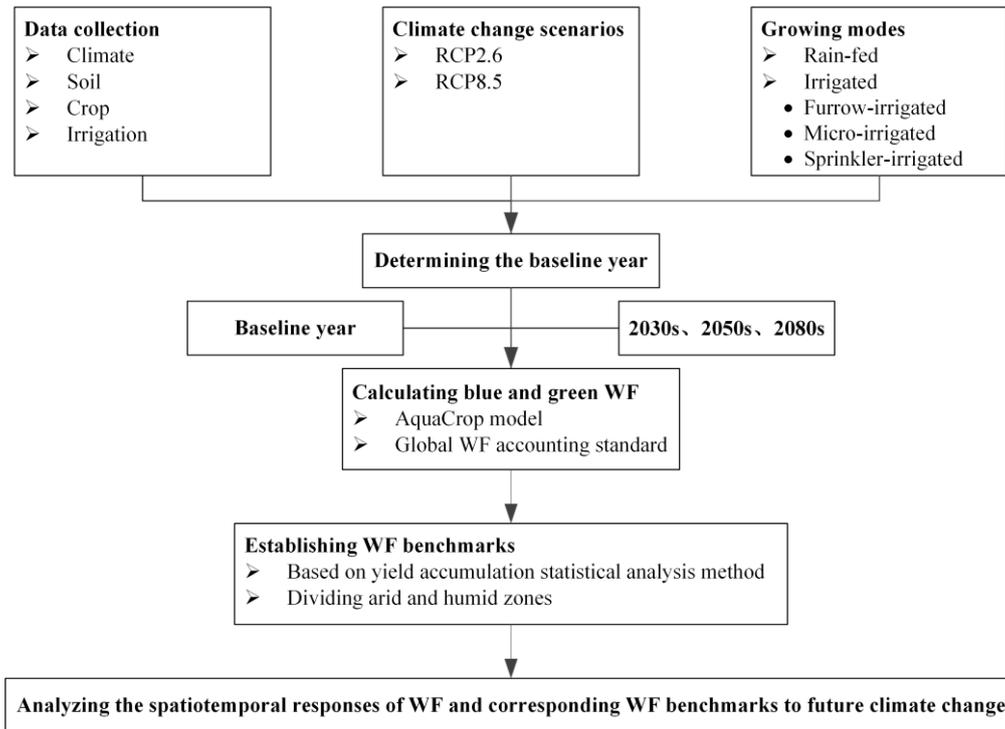
121 **Figure 1.** Flow chart for the study.

122

2.2 Determining the baseline year

124   Determining the baseline year is needed for a comparison between future and current conditions. Climate determines the
125 annual variability of WF (Zhuo et al., 2014), and the baseline year should be determined when there is a relative balance
126 between aridity and moisture. Hence, the aridity index (AI) was used here. Annual reference evapotranspiration (ET$_0$, mm)
127 and precipitation (PR, mm) in China were calculated (Harris et al., 2014). Then, the AI was calculated, and climate change
128 trends from 2000 to 2014 were analysed. The year 2013 was designated the baseline as its drought level was nearest the 15-
129 year national average. The AI was calculated according to the method of Middleton and Thomas (1997):

$$AI = \frac{PR}{ET_0},$$ (1)

2.3 Water footprint per unit crop calculation

131   WF (m^3 t^{-1}) comprises blue WF (WF$_b$, m^3 t^{-1}) and green WF (WF$_g$, m^3 t^{-1}):

$$WF = WF_b + WF_g,$$ (2)

where WF_b and WF_g were calculated as the quotient of the blue (CWU_b, m³ ha⁻¹) and green (CWU_g, m³ ha⁻¹) components of crop water use (CWU, m³ ha⁻¹) and crop yield (Y, t ha⁻¹), respectively. CWU_b and CWU_g were equivalent to the cumulation of daily evapotranspiration (ET, mm d⁻¹) throughout the whole crop growth period (Hoekstra et al., 2011):

$$WF_b = \frac{CWU_b}{Y} = \frac{10 \times \sum_{d=1}^{lgp} ET_b}{Y} , \tag{3}$$

$$WF_g = \frac{CWU_g}{Y} = \frac{10 \times \sum_{d=1}^{lgp} ET_g}{Y} , \tag{4}$$

where ET_b and ET_g (mm) refer to the blue and green water evapotranspiration, respectively, and lgp refers to the number of days of the crop growth period. The coefficient, 10, is a unit conversion factor, transforming the water depth of ET (mm) into the water amount per unit land area of CWU (m³ ha⁻¹).

The ET and Y per grid for each crop were simulated by the AquaCrop model based on the dynamic daily soil water balance (Mekonnen and Hoekstra, 2010):

$$S_{[t]} = S_{[t-1]} + PR_{[t]} + IRR_{[t]} + CR_{[t]} - ET_{[t]} - RO_{[t]} - DP_{[t]} , \tag{5}$$

where $S_{[t]}$ and $S_{[t-1]}$ (mm) refer to the water content in soil when the day, t, ends and begins, respectively; $PR_{[t]}$ (mm) is the amount of precipitation on day, t; $IRR_{[t]}$ (mm) is the amount of water used for irrigation; $CR_{[t]}$ (mm) is the capillary rise to the crop root zone from the shallow groundwater; $RO_{[t]}$ (mm) is the water lost by surface runoff due to precipitation; and $DP_{[t]}$ (mm) is the water lost by deep percolation caused by excessive precipitation or irrigation. It was assumed that $CR_{[t]} = 0$ as the ground water depth was > 1 m (Allen et al., 1998). $RO_{[t]}$ was calculated using the Soil Conservation Service curve-number (CN) equation (USDA, 1964; Rallison, 1980):

$$RO_{[t]} = \frac{(PR_{[t]} - I_a)^2}{PR_{[t]} + S - I_a} , \tag{6}$$

$$S = 254 \left(\frac{100}{CN} - 1 \right) , \tag{7}$$

where S (mm) is the potential maximum water storage, and I_a (mm) is the initial amount of water loss before the runoff formation.

By tracking the daily flow of water in and out of the crop root zone, we separated the daily blue and green soil water balances (Zhuo et al., 2016b):

$$S_{b[t]} = S_{b[t-1]} + \left(PR_{[t]} + IRR_{[t]} - RO_{[t]} \right) \times \frac{IRR_{[t]}}{PR_{[t]} + IRR_{[t]}} - \left(DP_{[t]} + ET_{[t]} \right) \times \frac{S_{b[t-1]}}{S_{[t-1]}} , \tag{8}$$

$$S_{g[t]} = S_{g[t-1]} + \left(PR_{[t]} + IRR_{[t]} - RO_{[t]} \right) \times \frac{PR_{[t]}}{PR_{[t]} + IRR_{[t]}} - \left(DP_{[t]} + ET_{[t]} \right) \times \frac{S_{g[t-1]}}{S_{[t-1]}} , \tag{9}$$

where $S_{b[t]}$ and $S_{b[t-1]}$ (mm) are the blue water content in soil when the day, t, ends and begins, respectively; and $S_{g[t]}$ and $S_{g[t-1]}$ (mm) are the green water content in soil when the day, t, ends and begins, respectively. It is assumed that the initial soil water content before the crop growth period is green water.

In AquaCrop, the daily transpiration ($Tr_{[t]}$, mm) calculates the daily shoot biomass production (B, kg) using the normalised crop biomass water productivity (WP^*, kg m⁻²) (Raes et al., 2017):

$$B=WP^*\times\sum\frac{Tr_{[t]}}{ET_{0[t]}},\qquad(10)$$

155   where WP^* is normalised to consider CO_2 concentration, reference evapotranspiration (ET_0), and crop classes (C3 or C4) so

156   that it is applicable to various locations and seasons. Water productivity remains constant for specific crops. Y, as the

157   harvestable portion of final B, is calculated by multiplying B with the adjusted reference Harvest Index (HI_0, %):

$$Y=f_{HI}\times HI_0\times B,\qquad(11)$$

158   where f_{HI} is a correction factor for HI_0. It considers the water and temperature stresses during the crop growth period. Being

159   consistent with the existing widely used scaling method (Mekonnen and Hoekstra, 2011; Zhuo et al., 2016b, 2016c, 2019;

160   Wang et al., 2019; Mialyk et al., 2022), the simulated Y per grid for each crop in 2013 was validated via scaling model

161   simulation outputs to correspond with the crop yield statistics data at the provincial level (NBSC, 2021). With the consistent

162   scaling factors for the Y simulation and crop parameters including the crop calendar, WP^*, HI_0, and the maximum root depth

163   which represent the existing agricultural production level, climate was the only variable for future scenario simulations.

164   In the simulation, different growing modes, namely rain-fed and three different irrigation techniques (furrow, micro, and

165   sprinkler irrigation), were considered. The irrigation schedule of three irrigation techniques in the model was the Generation

166   of Irrigation Schedule, namely the generation of an irrigation schedule by specifying a time and depth criterion for planning

167   or evaluating a potential irrigation strategy. The time criterion we used was Allowable depletion (%), namely the percentage

168   of the Readily Available soil Water (RAW) that can be depleted before irrigation water has to be applied. The depth criterion

169   we used was the Back to field capacity as the extra water on top of the amount of irrigation water required to bring the root

170   zone back to field capacity. The water quality was expressed by the Electrical conductivity (dS m^{-1}) of the irrigation water.

171   The soil surface wetted (%), an indicative value for the fraction of soil surface wetted, was used to select irrigation techniques.

172   Table 2 shows the parameters of three irrigation techniques (Raes et al., 2017). We can adjust the simulated ET and Y according

173   to the performance of the irrigation schedule.

174

175   **Table 2.** Parameters of three irrigation techniques.

Irrigation technique	From day	Time criterion	Depth criterion	Water quality	Soil surface wetted
		Allowable depletion	Back to field capacity	Electrical conductivity	
		(%)	(+/- mm)	(dS m^{-1})	(%)
Furrow	1	50	10	1.5	80
Micro	1	20	10	0	40
Sprinkler	1	50	10	1.5	100

176

177   **2.4 Benchmarking consumptive WF in crop production**

178   Based on the work of Mekonnen and Hoekstra (2014), we ranked grid-level WF for each crop in ascending order of size

179   against the corresponding cumulative percentages of the total crop production. The annual WF of 20 % or 25 % of the producers

180   with the highest water productivity in China was set as the annual WF benchmark. The climate zones should be divided when
181   WF benchmarks are established (Zhuo et al., 2016a). To this end, the AI partitioned China into arid (< 0.5) and humid (> 0.5)
182   zones based on the annual ET_0 and PR from 2000 to 2014 at a 30-arc minute grid resolution (Harris et al., 2014) (Fig. 2).
183

184
185   **Figure 2.** Regions and climate zones of mainland China.
186

2.5 Data sources

188   Monthly climate data, such as maximum (Tx), minimum air temperature (Tn), precipitation (PR), and reference
189   evapotranspiration (ET_0), from 2000 to 2014 at a resolution of 30-arc minute were derived from the CRU-TS 3.24 dataset
190   (Harris et al., 2014; CEDA, 2018). The mean annual atmospheric CO_2 concentration (ppm) from 2000 to 2014 was obtained
191   from the Mauna Loa Observatory, Hawaii, USA (NOAA, 2018). The downscaled outputs of six GCMs at a 5-arc minute grid
192   resolution in the 2030s, 2050s, and 2080s were obtained from the Climate Change, Agriculture and Food Security (CCAFS)
193   database (Navarro-Racines et al., 2020; CCAFS, 2015). As the CCAFS database has no ET_0 data, we calculated ET_0 for each
194   climate scenario using temperature inputs via the FAO Penman-Monteith method with missing data as described by Allen et
195   al. (1998). The projected CO_2 concentrations under RCP2.6 and RCP8.5 were obtained from van Vuuren et al. (2007) and
196   Riahi et al. (2007), respectively. To make the model simulation more in line with the actual situation in China, we reset the
197   maximum root depth (Z_x) according to the FAO-56 recommendation (Allan et al., 1998). The FAO-56 recommended values
198   provide clear range of the Z_x for each type of crops for typical climatic zones. In addition, we further combined the literature
199   research on maize and wheat in China to reset the HI_0 (Zhuo et al., 2016c). The other parameters used in AquaCrop were

derived from Raes et al. (2017). Soil texture data and soil water capacity data at a 5-arc minute grid resolution were acquired from the ISRIC Soil and Terrain database (Dijkshoorn et al., 2008) and ISRIC-WISE dataset (Batjes, 2012), respectively. The planted areas for each irrigated or rain-fed crop at a 5-arc minute grid resolution were acquired from the MIRCA2000 dataset (Portmann et al., 2010). We divided these planted areas into different parts subjected to various irrigation techniques using statistical yearbook data (NBSC, 2021). Provincial-level crop yield statistics data were procured from the National Bureau of Statistics of China (NBSC, 2021).

3 Results

3.1 Future climate change trends in maize and wheat planted areas

In the baseline year 2013, the average annual reference evapotranspiration (ET_0) and precipitation (PR) in the planted areas of two crops were 941 mm and 727 mm, respectively. Compared with the baseline level of 2013, the average annual ET_0 and PR in the planted areas of two crops will both increase under two RCPs, and the increase in ET_0 exceeded that of PR. ET_0 will increase by 17 % and 29 % under RCP2.6 and RCP8.5, respectively, until the 2080s. However, PR will increase by 8 % and 14 %, respectively. The increases under RCP8.5 (18–29 % and 3–14 % for ET_0 and PR, respectively) were much higher than those under RCP2.6 (16–17 % and 4–8 % for ET_0 and PR, respectively). Climate change will be relatively more intense under RCP8.5. The increases in ET_0 were concentrated from April to August (14–39 mm). The increases in PR were concentrated between June and August (8–20 mm and 12–28 mm, respectively). However, PR will decline in May, July, November, and December, and it will decline more in May ($\leq$ 9 mm until the 2030s) (Fig. 3a, b). Water and heat resources were unevenly distributed in the planted areas of the two crops in 2013. ET_0 was relatively higher in East Coast and North China. PR distribution was comparatively higher in the South and lower in the North (Fig. S4). Compared with 2013, ET_0 and PR for the most heavily planted areas will increase under both scenarios until the 2080s. The areas with a relatively greater increase in ET_0 were distributed mainly in Southwest and Northeast (Fig. 3c, e), and PR increased relatively faster in Northwest and Jing-Jin (Fig. 3d, f). ET_0 decreased mainly in Xinjiang and Inner Mongolia (Fig. 3c, e), and PR decreased mainly in Xinjiang, Tibet, Northeast, and South Coast (Fig. 3d, f). However, the areas where ET_0 decreased were 86–94 % smaller than those where PR decreased.
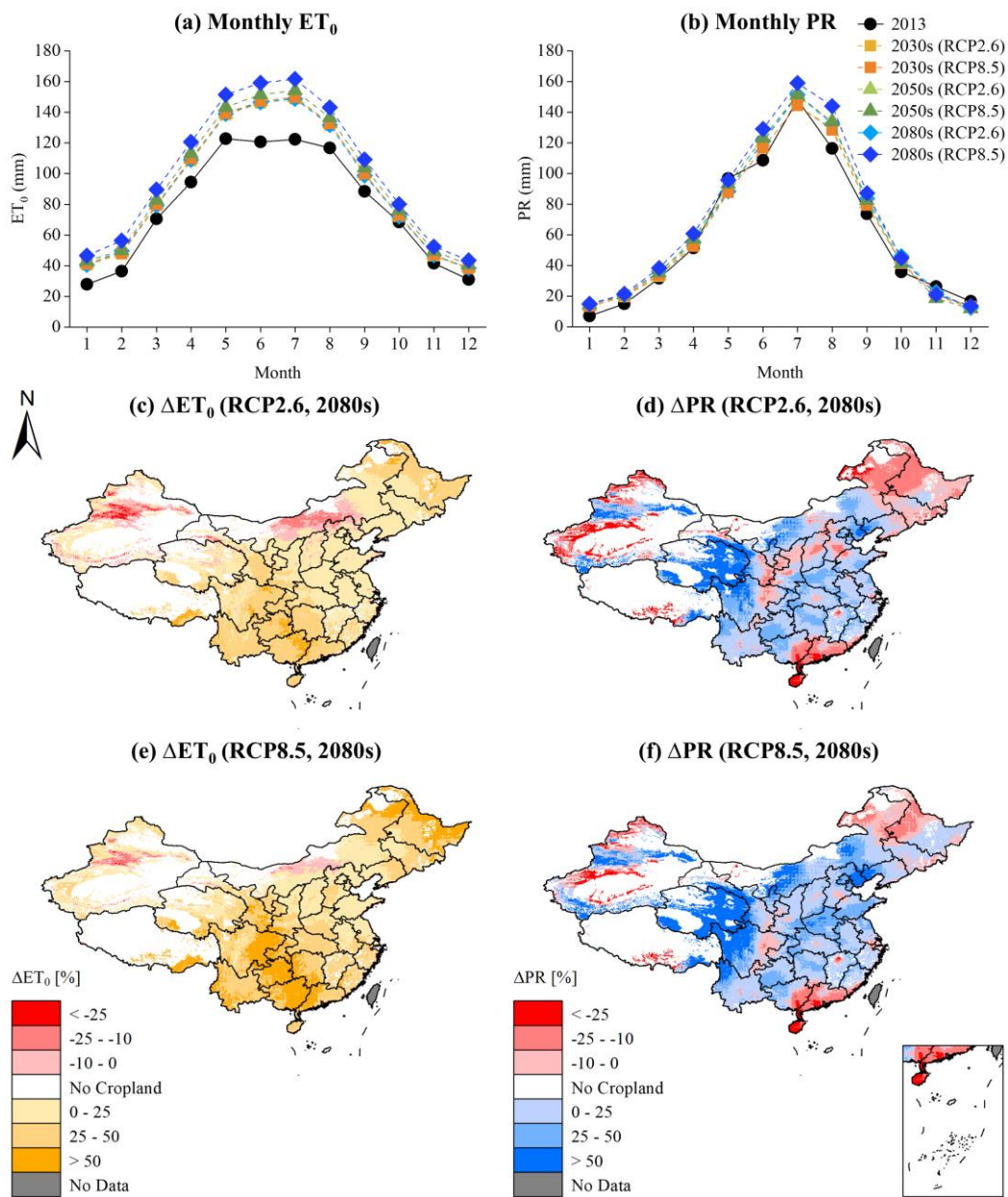
Figure 3. Future climate projections for the maize and wheat planted zones in China.

3.2 WF distribution in the baseline year 2013

The national average WF for wheat (1,008 m^3 t^{-1}) was higher than that for maize (813 m^3 t^{-1}) in the baseline year 2013. The corresponding blue WF proportions were 37 % and 20 %, respectively. The reason for this discrepancy is that maize is a C4 crop while wheat is a C3 crop. C4 crops have a relatively higher CO_2 fixation efficiency and faster photosynthetic rate than

232 C3 crops. Hence, maize can accumulate comparatively more yield than wheat under the same water consumption condition

233 (Wang et al., 2012). Figure 4 shows that the high WF_g value was mainly distributed in areas with relatively greater precipitation

234 during crop growth, i.e., abundant green water resources. The main component of WF is WF_g; therefore, the high maize WF

235 was mainly distributed in Northwest (Fig. 4a), while the high wheat WF was mainly distributed in Southwest and South Coast

236 (Fig. 4b). Elevated ET_0 and insufficient precipitation can increase blue water consumption in food production. Thus, the high

237 WF_b value was mainly distributed in areas with uneven water and heat resource distributions during crop growth. The high

238 maize WF_b was mainly distributed in Northwest and East Coast (Fig. 4c), while that of wheat was distributed mainly in North

239 China (Fig. 4d). In all grids, the proportions of WF_b and WF_g were up to 68 % (wheat in Xinjiang) (Table S2) and 98 % (maize

240 in Hainan) (Table S1), respectively.

241
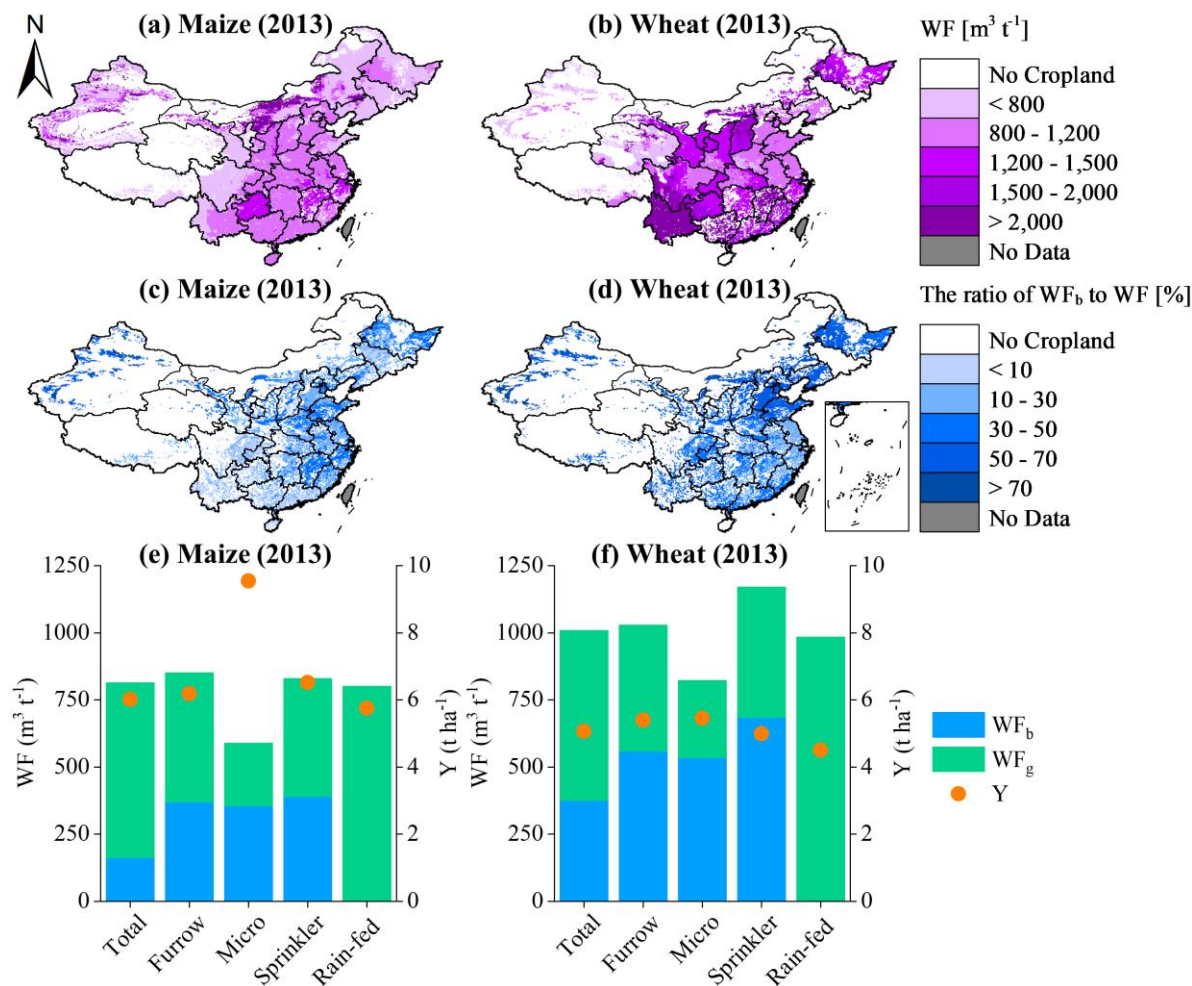
243 **Figure 4.** WF of maize and wheat in China in 2013.

244

245   A comparison of rain-fed and irrigation techniques demonstrated that the WF of maize and wheat under furrow and

246   sprinkler irrigation was higher than that under rain-fed in 2013. The WF of micro-irrigated crops was lower than that of rain-

247   fed crops. The WF of maize ($850 \, m^3 \, t^{-1}$) and wheat ($1,170 \, m^3 \, t^{-1}$) was highest under furrow and sprinkler irrigation, respectively.

248   For wheat under all three irrigation techniques, WF_b was dominant (54–65 %). However, WF_b for maize was only dominant

249   under micro irrigation (61 %). Micro-irrigated ($9.55 \, t \, ha^{-1}$ for maize and $5.46 \, t \, ha^{-1}$ for wheat) and rain-fed ($5.76 \, t \, ha^{-1}$ for

250   maize and $4.51 \, t \, ha^{-1}$ for wheat) crops had the highest and lowest yield, respectively, in 2013. The responses of maize yield to

251   rain-fed and various irrigation techniques were stronger than those of wheat yield (Fig. 4e, f).

252 3.3 Spatiotemporal responses of WF to future climate change

253   Compared with the baseline year 2013 and at the national average level, maize WF will increase under both RCP2.6 and

254   RCP8.5, by 17 % and 13 %, respectively, until the 2080s. The WF of wheat will increase under RCP2.6 (by 12 % until the

255   2080s) but decrease by 12 % under RCP8.5 until the 2080s (Fig. 5a). The increases in CO_2 concentration and, by extension,

256   yield gain, will be lower under RCP2.6 than RCP8.5. During the same period, the increases in WF under RCP2.6 will be 1–

257   3 % higher for maize and 2–10 % higher for wheat than those under RCP8.5. There will be relatively smaller differences in

258   CO_2 concentration between climate scenarios of the 2030s (431 ppm under RCP2.6 and 449 ppm under RCP8.5). Thus, the

259   differences in WF between RCPs will be smaller before the 2030s and larger after the 2050s. The WF of irrigated wheat under

260   RCP8.5 will decline by 3 % until the 2050s and by 15 % until the 2080s. The increase in WF will be highest under rain-fed,

261   and the WF of rain-fed maize and wheat under RCP2.6 will increase by 19 % and 24 %, respectively, until the 2080s. By

262   contrast, the WF of irrigated maize and wheat under RCP2.6 will only increase by 13 % and 7 %, respectively, until the 2080s

263   (Fig. 5a). A comparison of the various irrigation techniques demonstrated that the WFs of wheat and maize respond differently

264   under the same scenario. The increase in WF amplitude for maize will be highest under furrow irrigation (14 % and 11 %

265   under RCP2.6 and RCP8.5 until the 2080s, respectively) and lowest under micro irrigation (5 % and 2 % under RCP2.6 and

266   RCP8.5 until the 2080s, respectively). The WF of sprinkler-irrigated wheat under RCP8.5 will decline by 1 % until the 2030s.

267   The WF of wheat under micro irrigation had the highest increase (9 % until the 2080s under RCP2.6) and the lowest decrease

268   (14 % until the 2080s under RCP8.5). The WF of wheat under sprinkler irrigation had the lowest increase (only 2 % until the

269   2080s under RCP2.6) and the highest decrease (19 % until the 2080s under RCP8.5) (Fig. 5b).

270
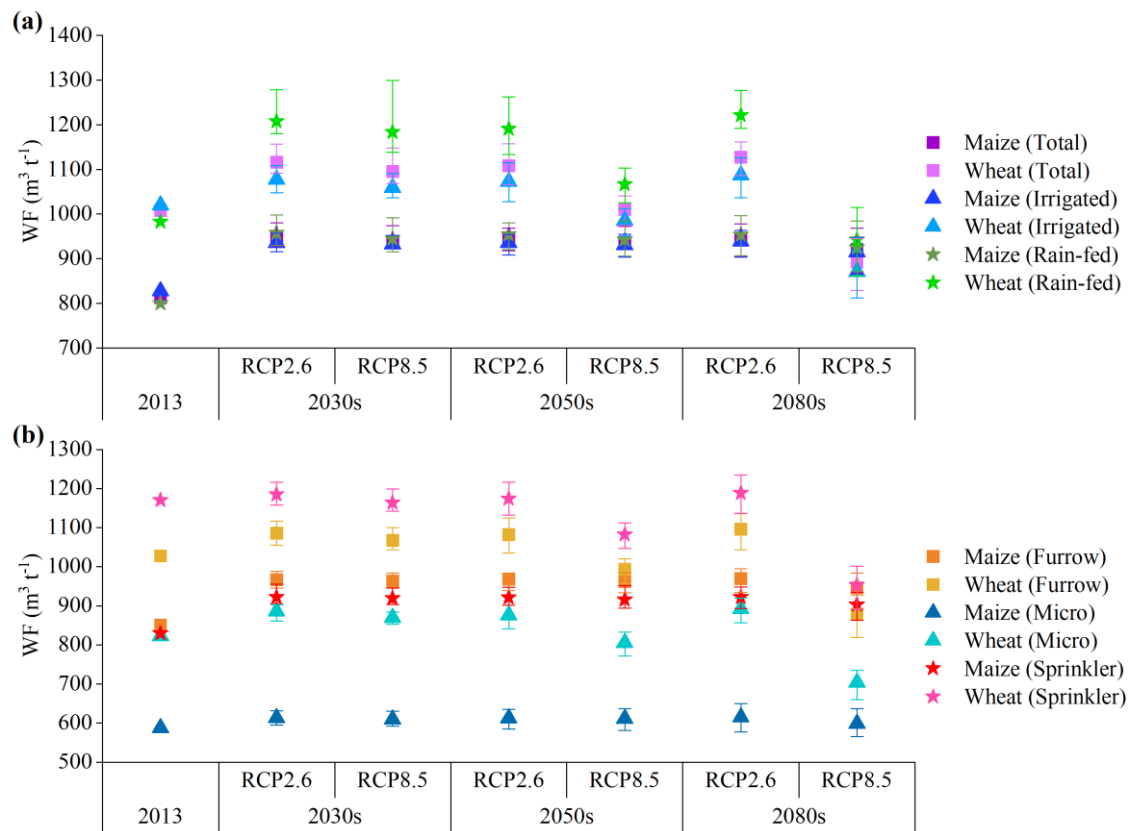
Figure 5. WF of maize and wheat in 2013 and future year levels under various climate change scenarios in China.

The spatial distribution of the relative changes in maize and wheat WF from 2013 to the 2080s showed regional differences. The WF will increase for 90–93 % of all areas planted with maize (Fig. 6a, b), and it will increase for 78 % of all areas planted with wheat under RCP2.6 (Fig. 6c) and decrease for 81 % of all areas planted with wheat under RCP8.5 (Fig. 6d). Increases in ET_0 lead to increases in WF, while decreases in PR lead to increases in WF_b (Fig. S6). Hence, the regions with relatively greater increases in WF were mainly distributed where ET_0 strongly increased and PR slightly increased or even decreased. In Yunnan, maize WF increased by 44 % and 38 % under RCP2.6 and RCP8.5, respectively. In Guangxi, wheat WF increased by 50 % and 16 % under RCP2.6 and RCP8.5, respectively (Table S5). Comparison of rain-fed and various irrigation techniques revealed that the WF of each crop responded uniquely to latitudinal and longitudinal climate change under the same scenario. The responses of maize WF to climate change with latitude were relatively consistent. It increased by 27–43 % at 19–26 °N and ~51 °N latitude and decreased at ~44 °N latitude. By contrast, the responses of WF for rain-fed maize were more sensitive at ~40 °N and ~52 °N latitude. The responses of maize WF vary widely within 74–100 °E longitude. The WF of maize under rain-fed and furrow and sprinkler irrigation declined at 74–90 °E longitude. The increase in WF for maize under rain-fed at 93–98 °E longitude was 3–51 % higher than the increase in WF for maize under furrow and

287   sprinkler irrigation. The WF of micro-irrigated maize decreased at 74–95 °E longitude (Fig. 6a, b). The responses of wheat

288   WF to climate change with latitude and longitude were relatively consistent. However, in certain areas, there were large

289   differences in wheat WF between rain-fed and the three irrigation techniques. The WF of wheat under rain-fed decreased at

290   74–80 °E longitude and by more than the WF of wheat under the three irrigation techniques at the same longitude range. The

291   increases in the WF of wheat under rain-fed at ~93 °E and ~122 °E longitude and ~22 °N latitude were significantly higher

292   than the increases in WF of wheat under the three irrigation techniques (Fig. 6c, d).

293
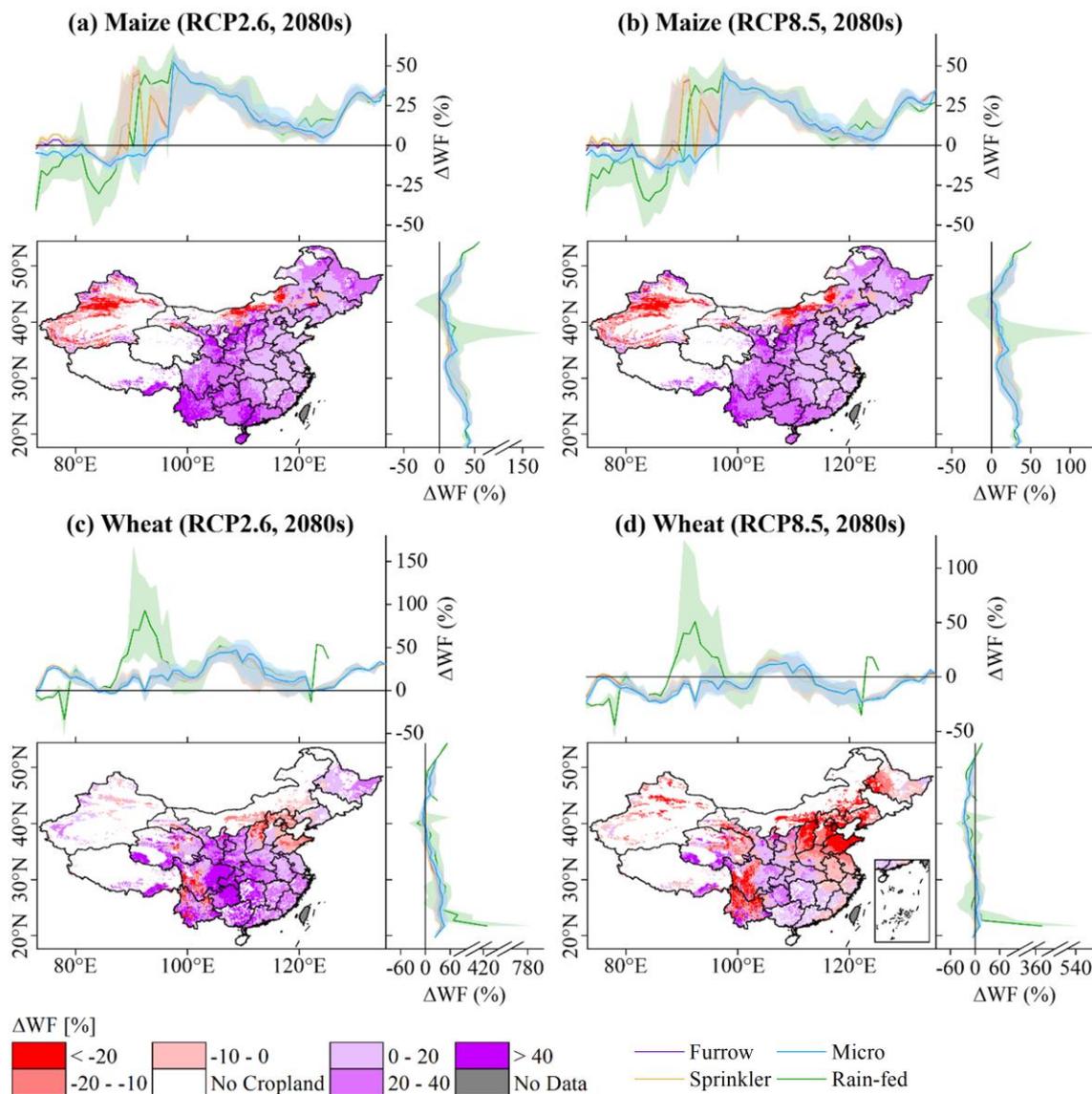
295   **Figure 6.** Spatial distributions in relative changes Δ (%) in WF (bottom left panel) with longitudinal (top panel) and latitudinal (right

296   panel) changes under different irrigation techniques applied to both crops under two scenarios from 2013 to the 2080s.

297

298   WF is determined by both crop yield (Y) and crop water use (CWU). We compared the relationships between the relative

299 changes in WF (ΔWF) and corresponding Y (ΔY) and CWU (ΔCWU) (Fig. 7). The ΔWF of maize and wheat under future

300 climate change scenarios was inversely proportional to ΔY and directly proportional to ΔCWU. Nevertheless, ΔWF was

301 relatively more sensitive to ΔY. When ΔY was 25 %, ΔWF of wheat under RCP2.6 and maize was approximately -25 %, while

302 ΔWF of wheat under RCP8.5 was approximately -10 %. When ΔCWU was 25 %, ΔWF of wheat under RCP2.6 and maize

303 was ~20 %, while ΔWF of wheat under RCP8.5 was approximately -8 % (Fig. 7a, b). The responses of ΔWF of maize were

304 more sensitive to ΔY and ΔCWU than those of wheat. The responses of ΔWF of maize and wheat under RCP2.6 were more

305 sensitive to ΔY and ΔCWU than those under RCP8.5. Comparison of rain-fed and various irrigation techniques revealed that

306 the correlation between ΔWF and ΔY was stronger for rain-fed crops. For rain-fed maize, R^2 can reach 0.55 (Fig. 7a). ΔWF

307 and ΔCWU were strongly correlated for irrigated crops, and ΔWF and ΔCWU were especially strongly correlated for crops

308 under micro irrigation (R^2 can reach 0.98 for wheat) (Fig. 7b). We also determined the relationship between ΔWF$_b$ and ΔCWU$_b$

309 was similar but more significant than that between ΔWF and ΔCWU (Fig. 7c).

310

311
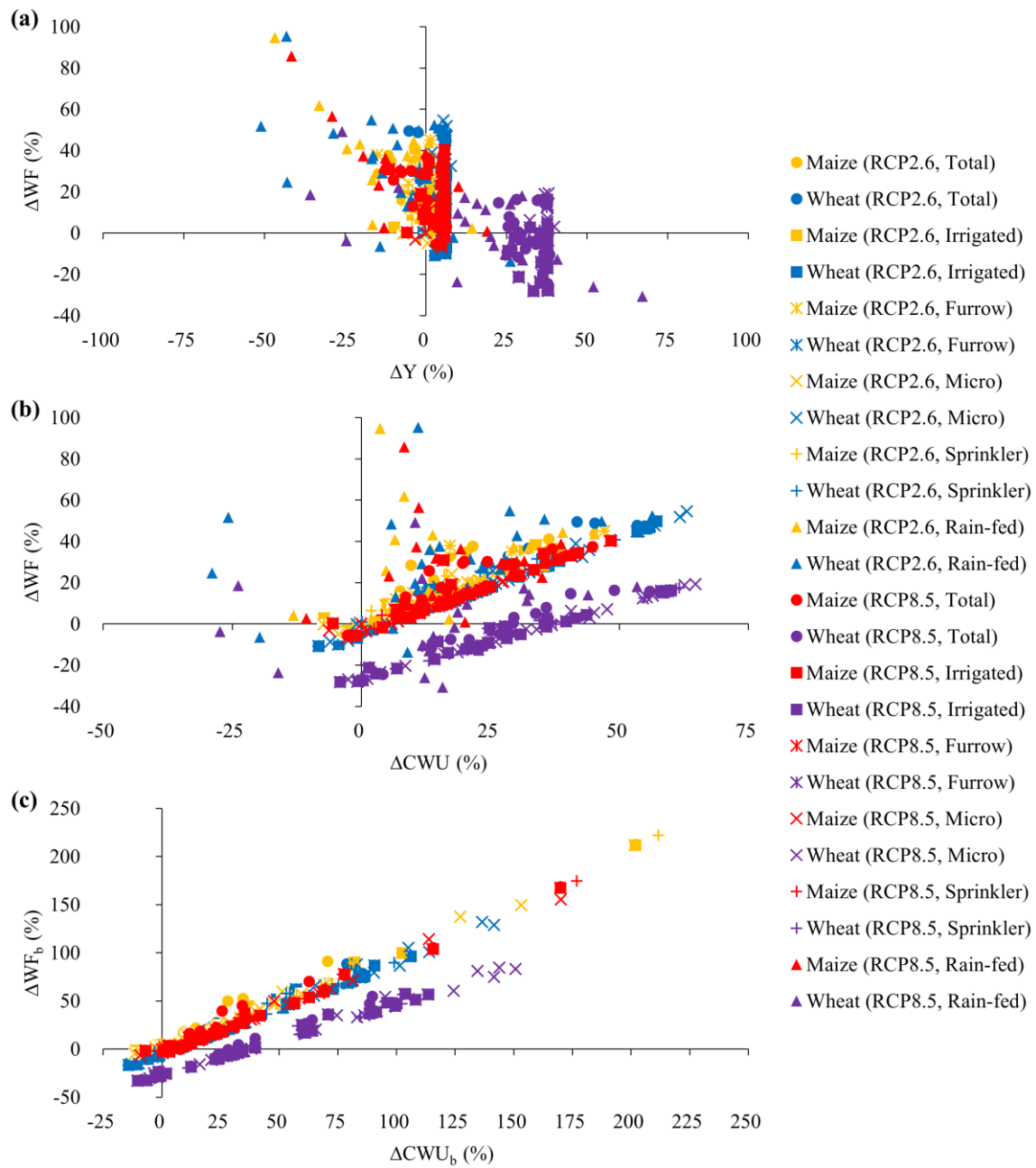
Figure 7. Relationships between relative changes Δ (%) in **(a)** Y and corresponding WF, **(b)** CWU and corresponding WF, and **(c)** CWU$_b$
313   and corresponding WF$_b$ of two crops under RCP2.6 and RCP8.5 from 2013 to the 2080s.

314

3.4 Spatiotemporal WF benchmarks responses to climate change

Table 3 shows the WF benchmarks of maize and wheat among various irrigation techniques and climate zones in 2013 and future year levels. The WF benchmarks of maize and wheat in the humid zone were 13–32 % higher than those in the arid zone, which is similar to results obtained by Wang et al. (2019). In the same climate zone, WF benchmarks of wheat were generally 2–35 % higher than those of maize. However, in the humid zone, the WF benchmark for the 25th production percentile of maize was 3 % higher than that of wheat under RCP8.5 in the 2080s. In the arid zone, WF benchmarks of rain-fed maize were 13–34 % higher than those of irrigated maize. In the humid zone of the future, WF benchmarks of rain-fed wheat were 2–7 % higher than those of irrigated wheat. In general, WF benchmarks of sprinkler-irrigated crops were higher, while those of micro-irrigated crops were lower. The differences in WF benchmarks among various irrigation techniques were more significant in the arid zone. WF benchmarks of the crops under micro irrigation were 30–38 % lower than those under sprinkler irrigation in the arid zone. The difference in the humid zone was only 8–14 %, which is also consistent with the study by Wang et al. (2019). In the humid zone, however, WF benchmarks of maize under furrow irrigation were 7–21 % higher than those under sprinkler irrigation.

Table 3. WF benchmarks (m^3 t^{-1}) of maize and wheat for different climate zones in 2013 and future year levels under two climate change scenarios in China.

Climate zones	Crop	Type	WF (m^3 t^{-1}) at different production percentile[*]					
			20th			25th		
			2013	RCP2.6	RCP8.5	2013	RCP2.6	RCP8.5
Arid	Maize	Total	601	(577, 576, 580)	(589, 584, 566)	623	(661, 658, 655)	(655, 652, 634)
		Irrigated	522	(505, 504, 506)	(503, 503, 496)	548	(508, 507, 511)	(507, 509, 501)
		Furrow	618	(658, 658, 658)	(654, 654, 642)	654	(693, 693, 691)	(689, 687, 674)
		Micro	466	(455, 454, 456)	(456, 454, 440)	477	(459, 458, 460)	(458, 460, 446)
		Sprinkler	700	(727, 725, 723)	(722, 719, 708)	706	(729, 729, 726)	(724, 721, 710)
		Rain-fed	599	(661, 661, 662)	(652, 649, 630)	618	(682, 679, 671)	(672, 667, 652)
	Wheat	Total	753	(776, 764, 781)	(765, 707, 620)	768	(829, 816, 828)	(809, 756, 666)
		Irrigated	754	(776, 764, 781)	(765, 707, 620)	768	(830, 816, 829)	(810, 757, 666)
		Furrow	830	(850, 840, 850)	(830, 774, 680)	940	(885, 875, 887)	(868, 809, 712)
		Micro	648	(701, 690, 705)	(694, 643, 562)	670	(717, 705, 721)	(707, 654, 572)
		Sprinkler	1020	(1003, 998, 1007)	(989, 920, 811)	1032	(1034, 1028, 1038)	(1019, 948, 837)
		Rain-fed	692	(743, 734, 753)	(729, 692, 618)	692	(790, 772, 791)	(769, 737, 653)
Humid	Maize	Total	680	(761, 754, 752)	(756, 752, 739)	718	(813, 807, 807)	(809, 806, 785)
		Irrigated	743	(905, 905, 908)	(902, 900, 881)	782	(939, 939, 944)	(937, 936, 916)
		Furrow	762	(925, 926, 930)	(921, 921, 901)	801	(943, 942, 948)	(940, 939, 919)
		Micro	649	(709, 704, 707)	(694, 696, 683)	660	(734, 726, 732)	(721, 726, 708)
		Sprinkler	713	(770, 771, 768)	(764, 762, 750)	737	(813, 814, 812)	(808, 806, 793)
		Rain-fed	631	(712, 703, 707)	(710, 702, 678)	656	(744, 737, 737)	(740, 736, 716)
	Wheat	Total	873	(933, 932, 946)	(921, 851, 752)	887	(944, 942, 957)	(931, 860, 760)

Irrigated	887	(914, 914, 924)	(900, 841, 744)	897	(925, 926, 937)	(912, 849, 752)
Furrow	887	(914, 914, 925)	(901, 841, 744)	896	(925, 927, 937)	(913, 849, 752)
Micro	820	(821, 826, 838)	(804, 753, 665)	833	(830, 839, 849)	(812, 759, 671)
Sprinkler	933	(949, 944, 955)	(936, 872, 770)	946	(958, 953, 964)	(944, 880, 777)
Rain-fed	812	(973, 958, 984)	(950, 863, 757)	831	(989, 973, 998)	(964, 877, 763)

*The three numbers in brackets are the values of 2030s, 2050s and 2080s.

Compared with the baseline year, 2013, the changes in maize and wheat WF benchmarks under future climate change scenarios are similar to the changes in WF. However, the WF benchmark for the 20th production percentile of maize will decline by 2–6 % in the arid zone. WF benchmarks of wheat under RCP8.5 will decrease by 2–6 % and 13–18 % until the 2050s and the 2080s, respectively. The increasing range of the WF benchmark for the 25th production percentile of maize was 7–8 % higher in the humid zone than that in the arid zone. The increasing range of the WF benchmark for the 20th production percentile of wheat was 4–5 % higher in the humid zone than that in the arid zone. WF benchmarks of maize and wheat increased to a greater extent under RCP2.6 but decreased to a greater extent under RCP8.5. WF benchmarks of rain-fed crops increased more than those of irrigated crops in the same climate zone. Nevertheless, the increase in WF benchmarks was 7–11 % lower for rain-fed than irrigated maize in the humid zone. WF benchmarks of maize and wheat generally increased relatively more under furrow irrigation and comparatively less under sprinkler irrigation. However, under RCP2.6, the growth rate of the WF benchmark for the 20th production percentile of wheat was 5–6 % higher under micro irrigation than that under furrow irrigation in the arid zone. The increase in the WF benchmark for the 20th production percentile of wheat was 0.19–2 % higher under sprinkler irrigation than that under micro irrigation in the humid zone (Table 3).

Figure 8 shows the spatial distribution of the relative changes in the WF of maize and wheat compared with the benchmark for the 25th production percentile in 2013 and the 2080s. In 2013, the WF for 81 % and 79 % of the maize and wheat planted areas, respectively, was higher than its benchmark. The maize planted areas with WF below the benchmark were distributed mainly in Xinjiang in the arid zone and northeast Inner Mongolia in the humid zone (Fig. 8a). The wheat planted areas with WF below the benchmark were distributed mainly in Xinjiang in the arid zone and Qinghai (Fig. 8d). Under future climate change scenarios, the maize and wheat planted areas with the WF below the benchmark will slightly decrease in the 2080s. These areas are mainly distributed in Heilongjiang, Tibet, southern Gansu, and Sichuan in the humid zone for maize; and Henan and Tibet in the humid zone and Qinghai for wheat. This is because that the annual ET_0 will increase relatively faster in Heilongjiang and Tibet, which will lead to a greater increase in WF_b. The annual PR in other regions will significantly increase, which will result in a greater increase in WF_g. Maize and wheat planted areas under RCP8.5 with WF below the benchmark will decrease by 5 % and 4 %, respectively, until the 2080s.
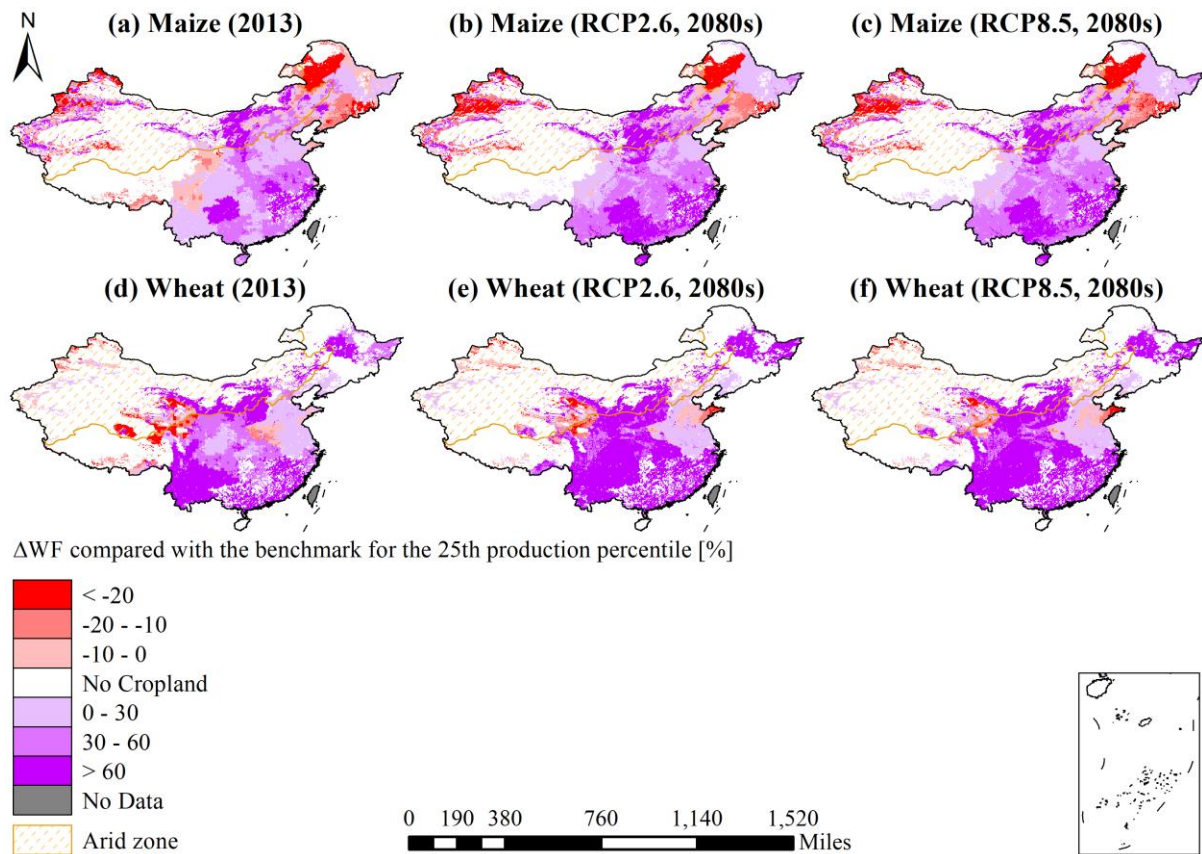
Figure 8. Relative changes Δ (%) in the WF of maize and wheat compared with the benchmark for the 25th production percentile in 2013 and the 2080s under RCP2.6 and RCP8.5 in different climate zones of China.

3.5 Discussion

This study analysed and compared the WF and WF benchmarks responses of wheat and maize under rain-fed and various irrigation conditions and forecasted their responses to future climate change scenarios in China. Under the background that the annual ET_0 and PR will both increase but ET_0 will increase faster, maize WF will increase under both RCP2.6 and RCP8.5. Wheat WF will increase under RCP2.6 but decrease under RCP8.5 until the 2080s. Rain-fed crops had higher ranges of increasing WF, which is consistent with Rosa et al. (2020). The increasing ranges of maize and wheat WF were lowest under micro irrigation and sprinkler irrigation, respectively. Therefore, the implementation of water-saving irrigation techniques (micro and sprinkler irrigation) may help mitigate the adverse effects of future climate change on agriculture, which is in line with Dai et al. (2020). Under future climate change, WF benchmarks will be modified in a manner resembling that for WF. However, the former changes will not be as significant as the latter in the same area.

In 2013, the WF of maize was lower than that of wheat. Nevertheless, maize WF is expected to increase more rapidly than wheat WF under future climate change scenarios. C4 crops such as maize have higher photosynthetic rates than C3 crops such as wheat. However, C4 crops are less sensitive to elevated atmospheric CO_2 than C3 crops (Bowes, 1993). Hence, while maize yield is higher than wheat yield, the former increases less than the latter. We compared current results against those of previous studies in Table 4. The differences we determined for the relative changes in maize and wheat WF between years and RCPs resembled those reported by Zhuo et al. (2016d). However, these authors also considered other factors, such as harvested crop area, technology, diet, and population, that could partially offset the adverse effects of future climate change. Therefore, maize and wheat WF will decline in the future according to Zhuo et al. (2016d). Fader et al. (2010) studied relative global-scale changes in maize WF for 2050. Their analysis was conducted in the opposite direction of that of the present study on China. Moreover, the two studies differed in terms of climate scenario, research area, and crop model. Winter wheat WF in Germany and Italy will decline by 2050 according to Garofalo et al. (2019). Nevertheless, our research showed that winter wheat WF will increase in China by 2050. The crop water use in Germany and Italy changes more smaller than that in China. However, our observed differences in the relative changes in WF between RCPs were consistent with those of Garofalo et al. (2019); namely, under RCP8.5, WF will either decrease more or increase less.

Table 4. Comparison of the results between current and previous studies.

Reference	Year	Study case	Scenario	Relative changes in WF (%)
Zhuo et al. (2016d)	2030	China Maize	RCP2.6 / RCP8.5	-38–-32 / -10–0
		China Wheat		-25–-17 / -20–-11
	2050	China Maize		-51–-43 / -22–-8
		China Wheat		-36–-27 / -38–-27
Current study	2030s (2020–2049)	China Maize	RCP2.6 / RCP8.5	17 / 16
		China Wheat		11 / 9
	2050s (2040–2069)	China Maize		16 / 15
		China Wheat		10 / 0.20
Fader et al. (2010)	2041–2070	Global Maize	SRES A2	-0.44–-0.35
Current study	2050s (2040–2069)	China Maize	RCP2.6 / RCP8.5	16 / 15
Garofalo et al. (2019)	2050	Germany Winter wheat	RCP4.5 / RCP8.5	-24 / -26
		Italy Winter wheat		-5 / -6
Current study	2050s (2040–2069)	China Winter wheat	RCP2.6 / RCP8.5	10 / 0.60

In the future, the spatial distributions of maize and wheat WF will change considerably. By contrast, the spatial distributions of WF benchmarks will negligibly change. This phenomenon is comparatively more pronounced in the area with limited agricultural development. In 2013, Guizhou and Guangxi had the highest maize and wheat WF (1,317 m^3 t^{-1} and 3,720 m^3 t^{-1}, respectively) (Table S1, S2). In the humid zone, maize WF in Guizhou and wheat WF in Guangxi will increase by 37 % and 50 %, respectively, under RCP2.6 and by 33 % and 16 %, respectively, under RCP8.5 until the 2080s (Table S5). Nevertheless, the WF benchmarks for the 25th production percentile of maize and wheat in the humid zone will only increase by 12 % and 8 %, respectively, under RCP2.6 and increase by 9 % and decrease by 14 %, respectively, under RCP8.5. These

areas will nonetheless have great potential for agricultural water conservation in the future. If maize and wheat WF in various regions of China can be reduced to the benchmark for the 25th production percentile, the total CWU can be reduced by 45–66 billion m^3 (~14–17 %). Rain-fed agriculture can save 27–40 billion m^3 (~18–22 %), water which is more than that conserved by irrigation. In irrigated agriculture, furrow irrigation has a comparatively high water-saving potential (17–22 billion m^3; ~11–12 %). To optimise the agricultural water-saving potential in China, we must either reduce WF or prevent it from increasing, either by enhancing crop yield or decreasing CWU. However, this goal can only be realised with the support of relevant policies and management practices. The annual PR is relatively low, and the ET$_0$ is relatively high in North China. Shortage of water for agriculture is a major bottleneck in the development of local agriculture there. However, furrow irrigation is mainly applied in these areas (Fig. S3). Hence, irrigation water use efficiency is low and WF$_b$ is high. High-efficiency, water-saving micro irrigation, and sprinkler irrigation could replace furrow irrigation in these areas so that CWU and WF decrease. The planted areas in the South have abundant precipitation but limited distribution (Fig. S2) and high WF (Fig. 4a, b). WF can be mitigated by implementing ground cover techniques (ex. straw return, mulch) to reduce soil evaporation and by improving farmer skills. WF can also be reduced by optimizing the structure of crop planting. Crops and varieties best adapted to local climate conditions and climate change can lower irrigation requirements and reduce WF.

To make climate models comparable and promote their development, The World Climate Research Program (WCRP) has developed and promoted the CMIP since 1995 (Meehl et al., 1997, 2000). Its current iteration is CMIP Phase 6 (CMIP6), which will be used in the forthcoming Intergovernmental Panel on Climate Change's Sixth Assessment Report (IPCC AR6). GCMs and their associated research results based on CMIP5 provided vital support for IPCC's Fifth Assessment Report (IPCC AR5). CMIP5 proposed four RCP scenarios (RCP2.6, RCP4.5, RCP6.0, and RCP8.5) by considering greenhouse gas (GHG) emissions and concentrations, atmospheric pollutant concentrations, and land use in the 21st century (Moss et al., 2008). However, no specific socio-economic assumptions were made. The Scenario Model Intercomparison Project (ScenarioMIP), as the primary activity within CMIP6, will provide a series of new climate scenarios that consider social factors related to climate change adaptation and impacts. They will be based on the combined application of shared socioeconomic pathways (SSPs) and RCPs and will compensate for the limitations of the RCPs in CMIP5 (O'Neill et al., 2016). The climate models in CMIP5 and CMIP6 can both effectively simulate changes in potential evapotranspiration (Liu et al., 2020) and precipitation (Müller et al., 2021) in most parts of the world. Müller et al. (2021) reported that CMIP5 and CMIP6 simulate increasing trends in temperature in a similar fashion. Nevertheless, the simulation generated by CMIP6 is higher than that by CMIP5. Notwithstanding, CMIP5 and CMIP6 are reasonably consistent and similar in terms of their abilities to predict future climate changes. This study focused on the responses of crop production to future climate change. It mainly considered the influences of GHG emission- and concentration-driven climate change and excluded the influences of alterations in socioeconomic development. Therefore, we implemented CMIP5 in our current research.

Three are two methods of establishing WF benchmarks (Hoekstra, 2013). Method 1 is based on yield accumulation statistical analysis. Due to the variability of WFs found across regions and among producers within a region, for each crop, we can select the WF of 20 % or 25 % of the producers with the highest water productivity as the WF benchmark (Mekonnen and

Hoekstra, 2014). Method 2 is based on the available optimal technique analysis. We can compare the WFs at each location under different agricultural management practices and take the WF associated with optimal practice, which results in the smallest WF, as the WF benchmark (Chukalla et al., 2015). Both methods establish WF benchmarks based on the maximum reasonable water consumption in each step of the product's supply chain (Hoekstra, 2014). Method 1 is suitable for large-scale application. The differences in environmental conditions (such as climate) and development conditions should be considered comprehensively (Mekonnen and Hoekstra, 2014; Zhuo et al., 2016a). The drawback of Method 1 is that no matter what spatial scope one takes in grouping producers, within that scope there will still be variability from place to place even if the differences in regional environmental and development conditions are taken into account (Schyns et al., 2022). Method 2 is suitable for smaller scale and overcomes this drawback of Method 1 to some extent. The Method 2's drawback is that it has the higher requirements on the setting and simulation of different agricultural management practices. We mainly want to explore the response of large-scale WF to future climate change under specific irrigation technique, that is, each irrigation technique has its corresponding WF benchmarks. And only one agricultural management practice, that is irrigation, is considered here. Therefore, we choose Method 1. A combination of methods should be established. If conditions permit, we strongly recommend that Method 1 and Method 2 are combined to establish small-scale WF benchmarks. Different agricultural management practices, such as irrigation, mulching techniques and so on, can be combined to further determine WF benchmarks.

The sources of uncertainty in research on the responses of crop production to climate change include GCMs, climate scenarios, crop models, and their interactions (Wang et al., 2020). Semenov and Stratonovitch (2010) proposed that the use of multiple GCMs can reduce the uncertainty associated with them. We selected three GCMs each for wet and dry climate outputs to encompass a broad climate prediction scenario. To objectively and comprehensively project the future climate change trends of China, we selected two extreme RCPs, namely, RCP2.6 and RCP8.5. Wang et al. (2020) suggested that crop models are the main source of uncertainty in predicting wheat yield in China under future climate change. The application of various crop models and parameter settings inevitably lead to different yield forecasts (Asseng et al., 2013). Hence, the use of AquaCrop alone may introduce uncertainty into WF forecasting.

The present study had certain limitations in terms of the assumptions it made for the simulation. First, we assumed that the crop parameters (such as planting calendar, HI_0, and Z_x) for each crop under the identical growing mode (irrigated or rain-fed) were constant on a spatiotemporal scale. Yoon and Choi (2020) proposed that future increases in temperature and precipitation might shorten the crop growth period. Xiao et al. (2020) indicated that the winter wheat and summer maize growing periods will be lengthened and shortened, respectively, under future climate change. However, we did not consider future changes in the crop growth period. Second, we assumed a constant soil surface moisture rate for each grid under the various irrigation techniques. Third, it was assumed that the observed changes in the planted areas in 2013 were based on the 2000 raster database, and we ignored the migration of planted areas. Finally, we assumed that the maize and wheat planted areas will not change in the future and would remain consistent with baseline year 2013. Thus, we did not consider future development of cultivated lands.

463   The core content of this study was to quantify the responses of maize and wheat WF and WF benchmarks to future climate
464   change under various irrigation techniques. Future research must improve the accuracy of the crop model simulation and
465   reduce the uncertainty of climate prediction associated with using different GCMs. Moreover, this study only considered future
466   climate change scenarios. Future investigations should also consider the influence of changes in technological development,
467   land use, growing modes, and so on.

468   **4 Conclusions**

469   This study explored the responses of maize and wheat WF accounting and benchmarking to future climate change in
470   China. The crops were subjected to various irrigation techniques. The year 2013 was the baseline, and WF and its benchmarks
471   were quantified for each crop under rain-fed and irrigation (furrow, micro, and sprinkler) management techniques in the 2030s,
472   2050s, and 2080s under RCP2.6 and RCP8.5 at a 5-arc grid scale. The AquaCrop model with the outputs of six GCMs in
473   CMIP5 as its input data was used to simulate the WF of maize and wheat. The results show that: (1) Compared with 2013, the
474   annual ET_0 and PR in the maize and wheat planted areas of China will both increase; however, the former will increase faster
475   than the latter. (2) Maize WF will increase under both RCP2.6 and RCP8.5 by 17 % and 13 %, respectively, until the 2080s.
476   Wheat WF will increase under RCP2.6 (by 12 % until the 2080s) but decrease by 12 % under RCP8.5 until the 2080s. Rain-
477   fed crops were more vulnerable to the adverse impacts of future climate change, and their WF increased to a greater extent
478   than that of irrigated crops. Micro irrigation and sprinkler irrigation resulted in the lowest increases in WF for maize and wheat,
479   respectively. Hence, these water-saving irrigation practices effectively mitigated the negative impact of climate change. (3)
480   Within different climate zones and under various irrigation techniques, there will be significant differences in the responses of
481   WF benchmarks to future climate change. The changes in WF and its benchmarks will be similar in response to future climate
482   change. The rate of increase in WF benchmarks for sprinkler-irrigated crops will generally be lower than those for rain-fed,
483   micro-irrigated, and furrow-irrigated crops within the same climate zone. However, the change in the spatial distribution of
484   WF benchmarks will not be as significant as that of WF itself. Moreover, this difference will be more pronounced in the region
485   with low agricultural development. Additionally, this study also demonstrated that the agricultural water in China still has
486   substantial water-saving potential and can be effectively conserved.

487

488   **Data availability.** Data sources are listed in Sect. 2.5. Data generated in this paper are available by contacting La Zhuo.

489   **Competing interests.** The authors declare that they have no conflict of interest.

Author contribution

La Zhuo and Pute Wu designed the study. Zhiwei Yue and Xiangxiang Ji carried it out, and prepared the manuscript with contributions from all co-authors.

Acknowledgements

The study is financially supported by the Program for Cultivating Outstanding Talents on Agriculture, Ministry of Agriculture and Rural Affairs, People's Republic of China [13210321], and the National Natural Science Foundation of China Grants [51809215].

References

Ahmadi, M., Etedali, H. R., and Elbeltagi, A.: Evaluation of the effect of climate change on maize water footprint under RCPs scenarios in Qazvin plain, Iran, Agr. Water Manage., 254, 106969, https://doi.org/10.1016/j.agwat.2021.106969, 2021.

Allen, R. G., Pereira, L. S., Raes, D., and Smith, M.: Crop evapotranspiration-Guidelines for computing crop water requirements-FAO Irrigation and drainage paper 56, 300, FAO, Rome, Italy, 1998.

Arora, V. K., Scinocca, J. F., Boer, G. J., Christian, J. R., Denman, K. L., Flato, G. M., Kharin, V. V., Lee, W. G., and Merryfield, W. J.: Carbon emission limits required to satisfy future representative concentration pathways of greenhouse gases, Geophys. Res. Lett., 38, 387–404, https://doi.org/10.1029/2010GL046270, 2011.

Arunrat, N., Pumijumnong, N., Sereenonchai, S., Chareonwong, U., and Wang, C.: Assessment of climate change impact on rice yield and water footprint of large-scale and individual farming in Thailand, Sci. Total Environ., 726, 137864, https://doi.org/10.1016/j.scitotenv.2020.137864, 2020.

Asseng, S., Ewert, F., Rosenzweig, C., Jones, J. W., Hatfield, J. L., Ruane, A. C., Boote, K. J., Thorburn, P. J., Rötter, R. P., Cammarano, D., Brisson, N., Basso, B., Martre, P., Aggarwal, P. K., Angulo, C., Bertuzzi, P., Biernath, C., Challinor, A. J., Doltra, J., Gayler, S., Goldberg, R., Grant, R., Heng, L., Hooker, J., Hunt, L. A., Ingwersen, J., Izaurralde, R. C., Kersebaum, K. C., Müller, C., Naresh Kumar, C., Nendel, C., O'Leary, G., Olesen, J. E., Osborne, T. M., Palosuo, T., Priesack, E., Ripoche, D., Semenov, M. A., Shcherbak, I., Steduto, P., Stöckle, C., Stratonovitch, P., Streck, T., Supit, I., Tao, F., Travasso, M., Waha, K., Wallach, D., White, J. W., Williams, J. R., and Wolf, J.: Uncertainty in simulating wheat yields under climate change, Nat. Clim. Chang., 3, 827–832, https://doi.org/10.1038/nclimate1916, 2013.

Bai, T. and Gao, J.: Optimization of the nitrogen fertilizer schedule of maize under drip irrigation in Jilin, China, based on DSSAT and GA, Agric Water Manag, 244, 106555, https://doi.org/10.1016/j.agwat.2020.106555, 2021.

Batjes, N.: ISRIC-WISE Derived Soil Properties on a 5 by 5 Arc-Minutes Global Grid (Ver. 1.2), ISRIC, Wageningen, The Netherlands, available at: https://www.isric.org, 2012.

Bowes, G.: Facing the Inevitable: Plants and Increasing Atmospheric CO2, Annu. Rev. Plant Phys. Plant Mol. Biol., 44, 309–332, https://doi.org/10.1146/annurev.pp.44.060193.001521, 1993.

CCAFS: CCAFS-Climate Statistically Downscaled Delta Method data, Climate Change, Agriculture and Food Security, available at: www.ccafs-climate.org, 2015.

CIDDC: China Irrigation and Drainage Development Center, China, available at: http://www.jsgg.com.cn/temp/Index/Display.asp?NewsID=12313, last access: 14 April 2022.

CEDA: Climatic Research Unit (CRU) time-series datasets of variations in climate with variations in other phenomena, NCAS British Atmospheric Data Centre, date of citation, available at: http://catalogue.ceda.ac.uk/uuid, 2018.

Chukalla, A. D., Krol, M. S., and Hoekstra, A. Y.: Green and blue water footprint reduction in irrigated agriculture: Effect of irrigation techniques irrigation strategies and mulching, Hydrol. Earth Syst. Sci., 19, 4877–4891, https://doi.org/10.5194/hess-19-4877-2015, 2015.

Dai, C., Qin, X. S., Lu, W. T., and Huang, Y.: Assessing adaptation measures on agricultural water productivity under climate change: A case study of Huai River Basin, China, Sci. Total Environ., 721, 137777, https://doi.org/10.1016/j.scitotenv.2020.137777, 2020.

Delworth, T. L., Broccoli, A. J., Rosati, A., Stouffer, R. J., Balaji, V., Beesley, J. A., Cooke, W. F., Dixon, K. W., Dunne, J., Dunne, K. A., Durachta, J. W., Findell, K. L., Ginoux, P., Gnanadesikan, A., Gordon, C. T., Griffies, S. M., Gudgel, R., Harrison, M. J., Held, I. M., Hemler, R. S., Horowitz, L. W., Klein, S. A., Knutson, T. R., Kushner, P. J., Langenhorst, A. R., Lee, H. C., Lin, S. J., Lu, J., Malyshev, S. L., Milly, P. C. D., Ramaswamy, V., Russell, J., Schwarzkopf, M. D., Shevliakova, E., Sirutis, J. J., Spelman, M. J., Stern, W. F., Winton, M., Wittenberg, A. T., Wyman, B., Zeng, F., and Zhang, R.: GFDL's CM2 Global Coupled Climate Models. Part I: Formulation and Simulation Characteristics, J. Clim., 19, 643–674, https://doi.org/10.1175/JCLI3629.1, 2006.

Dijkshoorn, J. A., Engelen, V. W. P. V., and Huting, J. R. M.: Soil and landform properties for LADA partner countries (Argentina, China, Cuba, Senegal, South Africa and Tunisia), ISRIC–World Soil Information and FAO, Wageningen, the Netherlands, available at: https://www.isric.org/, https://doi.org/10.13031/2013.42676, 2008.

Donner, L. J., Wyman, B. L., Hemler, R. S., Horowitz, L. W., Ming, Y., Zhao, M., Golaz, J. C., Ginoux, P., Lin, S. J., Schwarzkopf, M. D., Austin, J., Alaka, G., Cooke, W. F., Delworth, T. L., Freidenreich, S. M., Gordon, C. T., Griffies, S. M., Held, I. M., Hurlin, W. J., Klein, S. A., Knutson, T. R., Langenhorst, A. R., Lee, H. C., Lin, Y., Magi, B. I., Malyshev, S. L., Milly, P. C. D., Naik, V., Nath, M. J., Pincus, R., Ploshay, J. J., Ramaswamy, V., Seman, C. J., Shevliakova, E., Sirutis, J. J., Stern, W. F., Stouffer, R. J., Wilson, R. J., Winton, M., Wittenberg, A. T., and Zeng, F.: The Dynamical Core, Physical Parameterizations, and Basic Simulation Characteristics of the Atmospheric Component AM3 of the GFDL Global Coupled Model CM3, J. Clim., 24, 3484–3519, https://doi.org/10.1175/2011JCLI3955.1, 2011.

Dufresne, J. L., Foujols, M. A., Denvil, S., Caubel, A., Marti, O., Aumont, O., Balkanski, Y., Bekki, S., Bellenger, H., Benshila, R., Bony, S., Bopp, L., Braconnot, P., Brockmann, P., Cadule, P., Cheruy, F., Codron, F., Cozic, A., Cugnet, D., Noblet, N. D., Duvel, J. P., Ethé, C., Fairhead, L., Fichefet, T., Flavoni, S., Friedlingstein, P., Grandpeix, J. Y., Guez, L., Guilyardi,

554   E., Hauglustaine, D., Hourdin, F., Idelkadi, A., Ghattas, J., Joussaume, S., Kageyama, M., Krinner, G., Labetoulle, S.,

555   Lahellec, A., Lefebvre, M. P., Lefevre, F., Levy, C., Li, Z. X., Lloyd, J., Lott, F., Madec, G., Mancip, M., Marchand, M.,

556   Masson, S., Meurdesoif, Y., Mignot, J., Musat, I., Parouty, S., Polcher, J., Rio, C., Schulz, M., Swingedouw, D., Szopa,

557   S., Talandier, C., Terray, P., Viovy, N., and Vuichard, N.: Climate change projections using the IPSL-CM5 Earth System

558   Model: from CMIP3 to CMIP5, Clim. Dyn., 40, 2123–2165, https://doi.org/10.1007/s00382-012-1636-1, 2013.

559 Fader, M., Rost, S., Müller, C., Bondeau, A., and Gerten, D.: Virtual water content of temperate cereals and maize: Present

560   and potential future patterns, J. Hydrol., 384, 218–231, https://doi.org/10.1016/j.jhydrol.2009.12.011, 2010.

561 FAO: FAOSTAT on-line database, Food and Agriculture Organization of the United Nation, Rome, Italy, available at:

562   http://www.fao.org/faostat/en/#data/QC, 2021.

563 Garofalo, P., Ventrella, D., Kersebaum, K. C., Gobin, A., Trnka, M., Giglio, L., Dubrovský, M., and Castellini, M.: Water

564   footprint of winter wheat under climate change: Trends and uncertainties associated to the ensemble of crop models, Sci.

565   Total Environ., 658, 1186–1208, https://doi.org/10.1016/j.scitotenv.2018.12.279, 2019.

566 Guo, H., Li, S., Wong, F. L., Qin, S., Wang, Y., Yang, D., and Lam, H. M.: Drivers of carbon flux in drip irrigation maize

567   fields in northwest China, Carbon Balance Manag., 16, 12, https://doi.org/10.1186/s13021-021-00176-5, 2021.

568 Harris, I., Jones, P. D., Osborn, T. J., and Lister, D. H: Updated high-resolution grids of monthly climatic observations - the

569   CRU TS3.10 Dataset, Int. J. Climatol., 34, 623–642, https://doi.org/10.1002/joc.3711, 2014.

570 Hatfield, J. L. and Dold, C.: Water-Use Efficiency: Advances and Challenges in a Changing Climate, Front. Plant Sci., 10,

571   103, https://doi.org/10.3389/fpls.2019.00103, 2019.

572 Hoekstra, A. Y. (ed.): Virtual water trade: Proceedings of the International Expert Meeting on Virtual Water Trade, Delft, the

573   Netherlands, 12–13 December 2002, Value of Water Research Report Series No. 12, UNESCO-IHE, Delft, The

574   Netherlands, 2003.

575 Hoekstra, A. Y.: The water footprint of modern consumer society, Routledge, London, UK, 208 pp, 2013.

576 Hoekstra, A. Y.: Sustainable, efficient, and equitable water use: the three pillars under wise freshwater allocation, WIREs

577   Water, 1, 31–40, https://doi.org/10.1002/wat2.1000, 2014.

578 Hoekstra, A. Y., Chapagain, A. K., Aldaya, M. M., and Mekonnen, M. M.: The Water Footprint Assessment Manual: Setting

579   the Global Standard, Earthscan, London, UK, 2011.

580 Hurrell, J. W., Holland, M. M., Gent, P. R., Ghan, S., Kay, J. E., Kushner, P. J., Lamarque, J. F., Large, W. G., Lawrence, D.,

581   Lindsay, K., Lipscomb, W. H., Long, M. C., Mahowald, M., Marsh, D. R., Neale, R. B., Rasch, P., Vavrus, S., Vertenstein,

582   M., Bader, D., Collins, W. D., Hack, J. J., Kiehl, J., and Marshall, S.: The Community Earth System Model: A Framework

583   for Collaborative Research, Bull. Am. Meteorol. Soc., 94, 1339–1360, https://doi.org/10.1175/BAMS-D-12-00121.1,

584   2013.

585 IPCC: Summary for Policymakers. In: Climate Change 2021: The Physical Science Basis. Contribution of Working Group I

586   to the Sixth Assessment Report of the Intergovernmental Panel on Climate Change, edited by: Masson-Delmotte, V.,

587   Zhai, P., Pirani, A., Connors, S. L., Péan, C., Berger, S., Caud, N., Chen, Y., Goldfarb, L., Gomis, M. L., Huang, M.,

588 Leitzell, K., Lonnoy, E., Matthews, J. B. R., Maycock, T. K., Waterfield, T., Yelekçi, O., Yu, R., and Zhou, B., Cambridge
589 University Press, In Press, 2021.

590 Jans, Y., Bloh, W. V., Schaphoff, S., and Müller, C.: Global cotton production under climate change – Implications for yield
591 and water consumption, Hydrol. Earth Syst. Sci., 25, 2027–2044, https://doi.org/10.5194/hess-25-2027-2021, 2021.

592 Kappelle, M.: WMO Statement on the State of the Global Climate in 2019, World Meteorological Organization, Geneva,
593 Switzerland, 2020.

594 Karandish, F., Nouri, H., and Schyns, J. F.: Agricultural adaptation to reconcile food security and water sustainability under
595 climate change: the case of cereals in Iran, Earths Future, 10, e2021EF002095, https://doi.org/10.1029/2021EF002095,
596 2022.

597 Konapala, G., Mishra, A. K., Wada, Y., and Mann, M. E.: Climate change will affect global water availability through
598 compounding changes in seasonal precipitation and evaporation, Nat. Commun., 11, 3044,
599 https://doi.org/10.1038/s41467-020-16757-w, 2020.

600 Li, H., Mei, X., Nangia, V., Guo, R., Liu, Y., Hao, W., and Wang, J.: Effects of different nitrogen fertilizers on the yield,
601 water- and nitrogen-use efficiencies of drip-fertigated wheat and maize in the North China Plain, Agric Water Manag,
602 243, 106474, https://doi.org/10.1016/j.agwat.2020.106474, 2021.

603 Liu, X., Li, C., Zhao, T., and Han, L.: Future changes of global potential evapotranspiration simulated from CMIP5 to CMIP6
604 models, Atmos. Oceanic Sci Lett., 13, 568–575, https://doi.org/10.1080/16742834.2020.1824983, 2020.

605 Lobell, D. B. and Gourdji, S. M.: The influence of climate change on global crop productivity, Plant Physiol., 160, 1686–1697,
606 https://doi.org/10.1104/pp.112.208298, 2012.

607 Mali, S. S., Shirsath, P. B., and Islam, A.: A high-resolution assessment of climate change impact on water footprints of cereal
608 production in India, Sci. Rep., 11, 8715, https://doi.org/10.1038/s41598-021-88223-6, 2021.

609 Meehl, G. A., Boer, G. J., Covey, C., Latif, M., and Stouffer, R. J.: Intercomparison makes for a better climate model, Eos.
610 Trans. Amer. Geophys. Union, 78, 445–451, https://doi.org/10.1029/97EO00276, 1997.

611 Meehl, G. A., Boer, G. J., Covey, C., Latif, M., and Stouffer, R. J.: The Coupled Model Intercomparison Project (CMIP), Bull.
612 Am. Meteorol. Soc., 81, 313–318, https://doi.org/10.1175/1520-0477(2000)081<0313:TCMIPC>2.3.CO;2, 2000.

613 Mekonnen, M. M. and Hoekstra, A. Y.: A global and high-resolution assessment of the green, blue and grey water footprint
614 of wheat, Hydrol. Earth Syst. Sci., 14, 1259–1276, https://doi.org/10.5194/hess-14-1259-2010, 2010.

615 Mekonnen, M. M. and Hoekstra, A. Y.: The green, blue and grey water footprint of crops and derived crop products, Hydrol.
616 Earth Syst. Sci., 15, 1577-1600, https://doi.org/10.5194/hess-15-1577-2011, 2011.

617 Mekonnen, M. M. and Hoekstra, A. Y.: Water footprint benchmarks for crop production: A first global assessment, Ecol.
618 Indic., 46, 214–223, https://doi.org/10.1016/j.ecolind.2014.06.013, 2014.

619 Mialyk, O., Schyns, J. F., Booij, M. J., and Hogeboom, R. J.: Historical simulation of maize water footprints with a new global
620 gridded crop model ACEA, Hydrol. Earth Syst. Sci., 26, 923–940, https://doi.org/10.5194/hess-26-923-2022, 2022.

621 Middleton, N. and Thomas, D. S. G.: World atlas of desertification, Arnold, London, UK, 1997.

Moss, R., Babiker, M., Brinkman, S., Calvo, E., Carter, T., Edmonds, J., Elgizouli, I., Emori, S., Erda, L., Hibbard, K., Jones, R., Kainuma, M., Kelleher, J., Lamarque, J. F., Manning, M., Matthews, B., Meehl, J., Meyer, L., Mitchell, J., Nakicenovic, N., O'Neill, B., Pichs, R., Riahi, K., Rose, S., Runci, P., Stouffer, R., van Vuuren, D., Weyant, J., Wilbanks, T., van Ypersele, J. P., and Zurek, M.: Towards New Scenarios for Analysis of Emissions, Climate Change, Impacts, and Response Strategies, IPCC Expert Meeting Report, 19–21 September, 2007, Noordwijkerhout, Netherlands, Intergovernmental Panel on Climate Change (IPCC), Geneva, Switzerland, 132 pp, 2008.

Müller, C., Franke, J., Jägermeyr, J., Ruane, A. C., Elliott, J., Moyer, E., Heinke, J., Falloon, P. D., Folberth, C., Francois, L., Hank, T., César Izaurralde, R., Jacquemin, I., Liu, W., Olin, S., Pugh, T. A. M., Williams, K., and Zabel, F.: Exploring uncertainties in global crop yield projections in a large ensemble of crop models and CMIP5 and CMIP6 climate scenarios, Environ. Res. Lett., 16, 034040, https://doi.org/10.1088/1748-9326/abd8fc, 2021.

Myers, S. S., Smith, M. R., Guth, S., Golden, C. D., Vaitla, B., Mueller, N. D., Dangour, A. D., and Huybers, P.: Climate Change and Global Food Systems: Potential Impacts on Food Security and Undernutrition, Annu. Rev. Public Health, 38, 259–277, https://doi.org/10.1146/annurev-publhealth-031816-044356, 2017.

Navarro-Racines, C., Tarapues, J., Thornton, P., Jarvis, A., and Ramirez-Villegas, J.: High-resolution and bias-corrected CMIP5 projections for climate change impact assessments, Sci. Data, 7, 7, https://doi.org/10.1038/s41597-019-0343-8, 2020.

NBSC: National Data, China, National Bureau of Statistics, Beijing, China, available at: https://data.stats.gov.cn/, 2021.

NOAA: National Oceanic and Atmospheric Administration, U.S, available at: https://www.esrl.noaa.gov, 2018.

O'Neill, B. C., Tebaldi, C., van Vuuren, D. P., Eyring, V., Friedlingstein, P., Hurtt, G., Hurtt, R., Kriegler, E., Lamarque, J. F., Lowe, J., Meehl, G. A., Moss, R., Riahi, K., and Sanderson, B. M.: The Scenario Model Intercomparison Project (ScenarioMIP) for CMIP6, Geosci. Model Dev., 9, 3461–3482, https://doi.org/10.5194/gmd-9-3461-2016, 2016.

Pastor, A. V., Palazzo, A., Havlik, P., Biemans, H., Wada, Y., Obersteiner, M., Kabat, P., and Ludwig, F.: The global nexus of food–trade–water sustaining environmental flows by 2050, Nat. Sustain., 2, 499–507, https://doi.org/10.1038/s41893-019-0287-1, 2019.

Portmann, F. T., Siebert, S., and Döll, P.: MIRCA2000-Global monthly irrigated and rainfed crop areas around the year 2000: A new high-resolution data set for agricultural and hydrological modelling, Global Biogeochem. Cy., 24, https://doi.org/10.1029/2008gb003435, 2010.

Qiao, F., Song, Z., Bao, Y., Song, Y., Shu, Q., Huang, C., and Zhao, W.: Development and evaluation of an Earth System Model with surface gravity waves, J. Geophys. Res. Ocean., 118, 4514–4524, https://doi.org/10.1002/jgrc.20327, 2013.

Raes, D., Steduto, P., Hsiao, T. C., and Fereres, E.: Reference manual, Chapter 2, AquaCrop model, Version 6.0, Food and Agriculture Organization of the United Nations, Rome, Italy, 2017.

Rallison, R. E.: Origin and evolution of the SCS runoff equation, in: Symposium on Watershed Management, Boise, Idaho, United States, 21–23 July, 912–924, 1980.

Riahi, K., Gruebler, A., and Nakicenovic, N.: Scenarios of long-term socio-economic and environmental development under climate stabilization, Technol. Forecast. Soc. Chang., 74, 887–935, https://doi.org/10.1016/j.techfore.2006.05.026, 2007.

Rosa, L., Chiarelli, D. D., Sangiorgio, M., Beltran-Peña, A. A., Rulli, M. C., D'Odorico, P., and Fung, I.: Potential for sustainable irrigation expansion in a 3° C warmer climate, Proc. Natl. Acad. Sci. U. S. A., 117, 29526–29534, https://doi.org/10.1073/pnas.2017796117, 2020.

Schmidt, G. A., Kelley, M., Nazarenko, L., Ruedy, R., Russell, G. L., Aleinov, I., Bauer, M., Bauer, S. E., Bhat, M. K., Bleck, R., Canuto, V., Chen, Y. H., Cheng, Y., Clune, T. L., Genio, A. D., Fainchtein, R. D., Faluvegi, G., Hansen, J. E., Healy, R. J., Kiang, N. Y., Koch, D., Lacis, A. A., LeGrande, A. N., Lerner, J., Lo, K. K., Matthews, E. E., Menon, S., Miller, R. L., Oinas, V., Oloso, A. O., Perlwitz, J. P., Puma, M. J., Putman, W. M., Rind, D., Romanou, A., Sato, M., Shindell, D. T., Sun, S., Syed, R. A., Tausnev, N., Tsigaridis, K., Unger, N., Voulgarakis, A., Yao, M. S., and Zhang, J.: Configuration and assessment of the GISS ModelE2 contributions to the CMIP5 archive, J. Adv. Model. Earth Syst., 6, 141–184, https://doi.org/10.1002/2013MS000265, 2014.

Schmidt, G. A., Ruedy, R., Hansen, J. E., Aleinov, I., Bell, N., Bauer, M., Bauer, S., Cairns, B., Canuto, V., Cheng, Y., Delgenio, A. D., Faluvegi, G., Friend, A. D., Hall, T. M., Hu, Y., Kelley, M., Kiang, N. Y., Koch, D., Lacis, A. A., Lerner, J., Lo, K. K., Miller, R. L., Nazarenko, L., Oinas, V., Perlwitz, J., Perlwitz, J., Rind, D., Romanou, A., Russell, G. L., Sato, M., Shindell, D. T., Stone, P. H., Sun, S., Tausnev, N., Thresher, D., and Yao, M. S.: Present-Day Atmospheric Simulations Using GISS ModelE: Comparison to In Situ, Satellite, and Reanalysis Data, J. Clim., 19, 153–192, https://doi.org/10.1175/JCLI3612.1, 2006.

Schyns, J. F., Hogeboom, R. J., and Krol, M. S.: 4 - Water Footprint Assessment: towards water-wise food systems, in: Food Systems Modelling, edited by: Peters, C., and Thilmany, D., Academic Press, Salt Lake City, USA, 63–88, https://doi.org/10.1016/B978-0-12-822112-9.00006-0, 2022.

Semenov, M. A. and Stratonovitch, P.: Use of multi-model ensembles from global climate models for assessment of climate change impacts, Clim. Res., 41, 1–14, https://doi.org/10.3354/cr00836, 2010.

Tian, Y., Ruth, M., Zhu, D., Ding, J., and Morris, N.: A Sustainability Assessment of Five Major Food Crops' Water Footprints in China from 1978 to 2010, Sustainability, 11, 1–20, https://doi.org/10.3390/su11216179, 2019.

Trnka, M., Feng, S., Semenov, M. A., Olesen, J. E., Kersebaum, K. C., Rötter, R. P., Semerádová, D., Klem, K., Huang, W., Ruiz-Ramos, M., Hlavinka, P., Meitner, J., Balek, J., Havlík, P., and Büntgen, U.: Mitigation efforts will not fully alleviate the increase in water scarcity occurrence probability in wheat-producing areas, Sci. Adv., 5, eaau2406, https://doi.org/10.1126/sciadv.aau2406, 2019.

USDA: Estimation of direct runoff from storm rainfall, Section 4 Hydrology, Chapter 4, National Engineering Handbook, Washington DC, USA, 1–24, 1964.

van Vuuren, D. P., den Elzen, M. G. J., Lucas, P. L., Eickhout, B., Strengers, B. J., van Ruijven, B., Wonink, S., and van Houdt, R.: Stabilizing greenhouse gas concentrations at low levels: an assessment of reduction strategies and costs, Clim. Change, 81, 119–159, https://doi.org/10.1007/s10584-006-9172-9, 2007.

von Salzen, K., Scinocca, J. F., McFarlane, N. A., Li, J., Cole, J. N. S., Plummer, D., Verseghy, D., Reader, M. C., Ma, X., Lazare, M., and Solheim, L.: The Canadian Fourth Generation Atmospheric Global Climate Model (CanAM4). Part I: Representation of Physical Processes, Atmosphere-Ocean, 51, 104–125, https://doi.org/10.1080/07055900.2012.755610, 2013.

Wang, B., Feng, P., Liu, D. L., O'Leary, G. J., Macadam, I., Waters, C., Asseng, S., Cowie, A., Jiang, T., Xiao, D., Ruan, H., He, J., and Yu, Q.: Sources of uncertainty for wheat yield projections under future climate are site-specific, Nat. Food., 1, 720–728, https://doi.org/10.1038/s43016-020-00181-w, 2020.

Wang, C., Guo, L., Li, Y., and Wang, Z.: Systematic Comparison of C3 and C4 Plants Based on Metabolic Network Analysis, BMC Syst Biol., 6, S9, https://doi.org/10.1186/1752-0509-6-S2-S9, 2012.

Wang, J., Gao, S., Xu, Y., and Wang, H.: Application and Existing Problems of Drip Irrigation for Wheat in Xinjiang, in: 2011 International Conference on Agricultural and Natural Resources Engineering (ANRE 2011), Intelligent Information Technology Application Association, Singapore, 3 July 2011, 25–29, 2011.

Wang, W., Zhuo, L., Li, M., Liu, Y., and Wu, P.: The Effect of Development in Water-Saving Irrigation Techniques on Spatial-Temporal Variations in Crop Water Footprint and Benchmarking, J. Hydrol., 577, 123916, https://doi.org/10.1016/j.jhydrol.2019.123916, 2019.

Xiao, D., Liu, D. L., Wang, B., Feng, P., Bai, H., and Tang, J.: Climate change impact on yields and water use of wheat and maize in the North China Plain under future climate change scenarios, Agr. Water Manage., 238, 106238, 2020.

Xu, Z., Chen, X., Wu, S. R., Gong, M., Du, Y., Wang, J., Li, Y., and Liu, J.: Spatial-temporal assessment of water footprint, water scarcity and crop water productivity in a major crop production region, J. Clean. Prod., 224, 375–383, https://doi.org/10.1016/j.jclepro.2019.03.108, 2019.

Yoon, P. R. and Choi, J. Y.: Efects of shift in growing season due to climate change on rice yield and crop water requirements, Paddy Water Environ., 18, 291–307, https://doi.org/10.1007/s10333-019-00782-7, 2020.

Zain, M., Si, Z., Chen, J., Mehmood, F., Rahman, S. U., Shah, A. N., Li, S., Gao, Y., and Duan, A.: Suitable nitrogen application mode and lateral spacing for drip-irrigated winter wheat in North China Plain, PLoS One, https://doi.org/10.1371/journal.pone.0260008, 2021.

Zheng, J., Wang, W., Ding, Y., Liu, G., Xing, W., Cao, X., and Chen, D.: Assessment of climate change impact on the water footprint in rice production: Historical simulation and future projections at two representative rice cropping sites of China, Sci. Total Environ., 709, 136190, https://doi.org/10.1016/j.scitotenv.2019.136190, 2020.

Zhuo, L., Liu, Y., Yang, H., Hoekstra, A. Y., Liu, W., Cao, X., Wang, M., and Wu, P.: Water for maize for pigs for pork: An analysis of inter-provincial trade in China, Water Res., 166, 115074, https://doi.org/10.1016/j.watres.2019.115074, 2019.

Zhuo, L., Mekonnen, M. M., and Hoekstra, A. Y.: Sensitivity and uncertainty in crop water footprint accounting: a case study for the Yellow River basin, Hydrol. Earth Syst. Sci., 18, 2219–2234, https://doi.org/10.5194/hess-18-2219-2014, 2014.

721   Zhuo, L., Mekonnen, M. M., and Hoekstra, A. Y.: Benchmark levels for the consumptive water footprint of crop production

722   for different environmental conditions: a case study for winter wheat in China, Hydrol. Earth Syst. Sci., 20, 4547–4559,

723   https://doi.org/10.5194/hess-20-4547-2016, 2016a.

724   Zhuo, L., Mekonnen, M. M., Hoekstra, A. Y., and Wada, Y.: Inter- and intra-annual variation of water footprint of crops and

725   blue water scarcity in the Yellow River basin (1961–2009), Adv. Water Resour., 87, 29–41,

726   https://doi.org/10.1016/j.advwatres.2015.11.002, 2016b.

727   Zhuo, L., Mekonnen, M. M., and Hoekstra, A. Y.: The effect of inter-annual variability of consumption, production, trade and

728   climate on crop-related green and blue water footprints and inter-regional virtual water trade: A study for China (1978-

729   2008), Water Res., 94, 73–85, https://doi.org/10.1016/j.watres.2016.02.037, 2016c.

730   Zhuo, L., Mekonnen, M. M., and Hoekstra, A. Y.: Consumptive water footprint and virtual water trade scenarios for China —

731   With a focus on crop production, consumption and trade, Environ. Int., 94, 211–223,

732   https://doi.org/10.1016/j.envint.2016.05.019, 2016d.